CZECH TECHNICAL UNIVERSITY IN PRAGUE

Faculty of Electrical Engineering

MASTER'S THESIS

High Frequency Oscillation Analysis in Malformation Cortical Development Patients

Martin Dostál

May 2018

Department of Radio Engineering

Thesis supervisor: Ing. Petr Ježdík Ph.D.

Author statement for undergraduate thesis

I declare that the presented work was developed independently and that I have listed all sources of information used within it in accordance with the methodical instructions for observing the ethical principles in the preparation of university theses.

Prague, date..... .....

Prohlášení autora práce

Prohlašuji, že jsem předloženou práci vypracoval samostatně a že jsem uvedl veškeré použité informační zdroje v souladu s Metodickým pokynem o dodržování etických principů při přípravě vysokoškolských závěrečných prací.

V Praze dne..... .....

ZADÁNÍ DIPLOMOVÉ PRÁCE

I. OSOBNÍ A STUDIJNÍ ÚDAJE

Příjmení: **Dostál** Jméno: **Martin** Osobní číslo: **424801**

Fakulta/ústav: **Fakulta elektrotechnická**

Zadávající katedra/ústav: **Katedra radioelektroniky**

Studijní program: **Elektronika a komunikace**

Studijní obor: **Audiovizuální technika a zpracování signálů**

II. ÚDAJE K DIPLOMOVÉ PRÁCI

Název diplomové práce:

Analýza vysokofrekvenčních oscilací pacientů s vývojovými vadami mozku

Název diplomové práce anglicky:

High Frequency Oscillation Analysis in Malformation Cortical Development Patients

Pokyny pro vypracování:

Nad předloženým souborem pacientů s fokální kortikální dysplázií (FCD) proveďte kvantitativní a kvalitativní hodnocení výskytu fenoménu vysokofrekvenčních oscilací (HFO) ve skalpovém elektroencefalogramu.
Popište vztah výskytu HFO detekovaném současně v invazivním a skalpovém záznamu.
Navrhněte systém třídění HFO podle časové souvislosti s interiktálními výboji (IED).
Podle kvantitativních a kvalitativních parametrů HFO se pokuste rozlišit pacienty podle typu FCD

Seznam doporučené literatury:

[1] ROEHRI, Nicolas, et al. High-frequency oscillations are not better biomarkers of epileptogenic tissues than spikes. Annals of neurology, 2018, 83.1: 84-97.
[2] ANDRADE-VALENCA, L. P., et al. Interictal scalp fast oscillations as a marker of the seizure onset zone. Neurology, 2011, WNL. 0b013e318228bee2.
[3] JACOBS, Julia, et al. Interictal high-frequency oscillations (80–500 Hz) are an indicator of seizure onset areas independent of spikes in the human epileptic brain. Epilepsia, 2008, 49.11: 1893-1907.
[4] ENGEL JR, Jerome, et al. High-frequency oscillations: what is normal and what is not?. Epilepsia, 2009, 50.4: 598-604.

Jméno a pracoviště vedoucí(ho) diplomové práce:

Ing. Petr Ježdík, Ph.D., katedra měření, katedra teorie obvodů, LVR

Jméno a pracoviště druhé(ho) vedoucí(ho) nebo konzultanta(ky) diplomové práce:

Datum zadání diplomové práce: **01.02.2019** Termín odevzdání diplomové práce: **24.05.2019**

Platnost zadání diplomové práce: **20.09.2020**

Ing. Petr Ježdík, Ph.D. podpis vedoucí(ho) práce	prof. Mgr. Petr Páta, Ph.D. podpis vedoucí(ho) ústavu/katedry	prof. Ing. Pavel Ripka, CSc. podpis děkana(ky)

III. PŘEVZETÍ ZADÁNÍ

Diplomant bere na vědomí, že je povinen vypracovat diplomovou práci samostatně, bez cizí pomoci, s výjimkou poskytnutých konzultací. Seznam použité literatury, jiných pramenů a jmen konzultantů je třeba uvést v diplomové práci.

. | Podpis studenta

Datum převzetí zadání

Acknowledgments

I would like to thank my supervisor Petr Ježdík for his help, guidance and detailed consultations over the course of last year during my work on my master's thesis. Furthermore, I would like to thank the medical professionals at FN Motol child neurology department for providing the data necessary for this thesis.

Abstract

High Frequency Oscillations (HFOs) are a fairly new epilepsy biomarker that hasn't been properly assessed and defined yet. In this thesis, the presence of HFOs in scalp EEG recordings, gathered from a cohort of patients being treated in FN Motol hospital, was evaluated. For the evaluation to take place, a battery of new analytic methods was created, including HFO detector utilizing an unusual signal phase-based approach. With the help of these tools, an assessment of the temporal relationship between traditionally used Interictal Epileptic Discharges (IEDs) and the HFOs took place. In addition, an analysis of the propagation of HFOs recorded with intracranial electrodes to the scalp electrodes was made.

Keywords: HDEEG, scalp EEG, epilepsy, HFO, signal processing

Abstrakt

High Frequency Oscillations (HFOs) jsou relativně novou skupinou biomarkerů, která ještě není zcela přesně definovaná a je předmětem aktivního výzkumu. Tato práce se zabývá analýzou a vyhodnocením HFO v EEG záznamech získaných z pacientů vyšetřovaných v zařízení FN Motol. Byla vytvořena celá řada nových nástrojů a metod, včetně detektoru HFO, jehož funkce je založena na fázové informaci EEG signálu. Za použití zmíněných nástrojů byl zhodnocen časový vztah mezi tradičně používaným biomarkerem Interictal Epileptic Discharge (IEDs) a biomarkerem HFO. Dále byla provedena analýza šíření HFO z vnitřku mozku na skalp.

Klíčová slova: HDEEG, skalpové EEG, epilepsie, HFO, zpracování signálu

Contents

Table of figures

1 Introduction

Epilepsy is a neurological brain disorder, which can be characterized and manifests itself by epileptic seizures [1]. Refractory epilepsy is a type of epilepsy, which cannot be successfully treated by seizure medication. Many possible causes for epilepsy disorders exist – one of them is the *Malformation of cortical development* (MCD). MCD diagnosis is frequently associated with refractory epilepsy. Estimates are, that around 40% of children with refractory epilepsy show signs of cortical malformations [2]. This work focuses on *Focal cortical dysplasia* (FCD) - one specific type of abnormal neurogenesis which can be put under the umbrella term of MCD.

In some cases of epileptic patients, there is a possibility of curing the patient, by performing a resection surgery of a patient-specific part of the epileptic region of the brain. The scale and execution of this surgical procedure are based on multiple pieces of information, which include the results of an EEG analysis of a given patient.

The EEG analysis traditionally focuses on *Interictal epileptiform discharges* (IED) – a biomarker, which can be seen in the EEG recording as a sharp transient spike. In the last few years, there has been a discussion regarding another EEG phenomenon and its connection to the disorder. These phenomena are called *High frequency oscillations* (HFO) and these are the object of focus in this work.

The goals of this work have been set up as follows:

1. Assess HFOs in the provided patient's datasets
2. Assess HFO occurrence in simultaneous intracranial and scalp EEG recording
3. Design a scheme for classification of HFOs based on their temporal relation to IEDs
4. Try to estimate FCD type based on patient's HFO characteristics

2 Theoretical background

2.1 Electroencephalography

Electroencephalography (EEG) is a method of monitoring electric potentials generated by the brain. It uses multiple electrodes to sense and compare electric potentials to some referential level. This recording gathered by a given number of electrodes (channels) then creates an electric potential map. Important general EEG characteristics include:

1. Temporal sampling frequency – determines maximal recordable frequency according to the Nyquist – Shannon sampling theorem [3]

$$Bandwidth = \frac{fs}{2}$$

2. Spatial sampling frequency – insufficient spatial sampling can lead to a detection miss of some important event. Various specific events require various spatial sampling frequencies, e.g. for IEDs, the gain starts to diminish after using more than 64 electrodes [4].
3. Electrode size – differently sized electrodes monitor neuron populations of different sizes – small intracranial microelectrodes sense neuron population in a much smaller area than macroelectrodes which sense much larger neural area overall. This creates an effect of different "sensitivity" – smaller neural population can create electrical activity, which can be diminished on a larger scale thanks to the superposition of other neighboring neural populations [5].

Patients with more complicated cases of epilepsy first undergo the scalp EEG examination, which's results are then used for implantation of the intracranial SEEG/ECoG (described more thoroughly in the next chapters) as the approximate area of epileptic tissue has to be known in order to properly set up the intracranial electrodes.

2.1.1 Scalp EEG

Scalp EEG is a type of EEG, where the electric potentials generated by the brain are recorded by electrodes which are in direct contact with the patient's scalp skin. That means that the EEG signal is considerably attenuated because it has to go through layers of various tissue, including the skull, before coming into contact with the recording electrodes. Its main advantage lies in providing global information concerning the electric potential of the brain as opposed to the intracranial EEG montages. Scalp EEG's main disadvantage is much lower SNR in comparison to iEEG techniques and much more prominent disturbance of the signal by EMG signals.

2.1.1.1 Classical 10-20

The 10-20 system is a standard basic EEG examination montage. It can provide some localization information, but given its very low spatial sampling frequency, it is much better suited just for basic neurological/epilepsy diagnosis. The 10-20 montage consists of 21 electrodes [6].

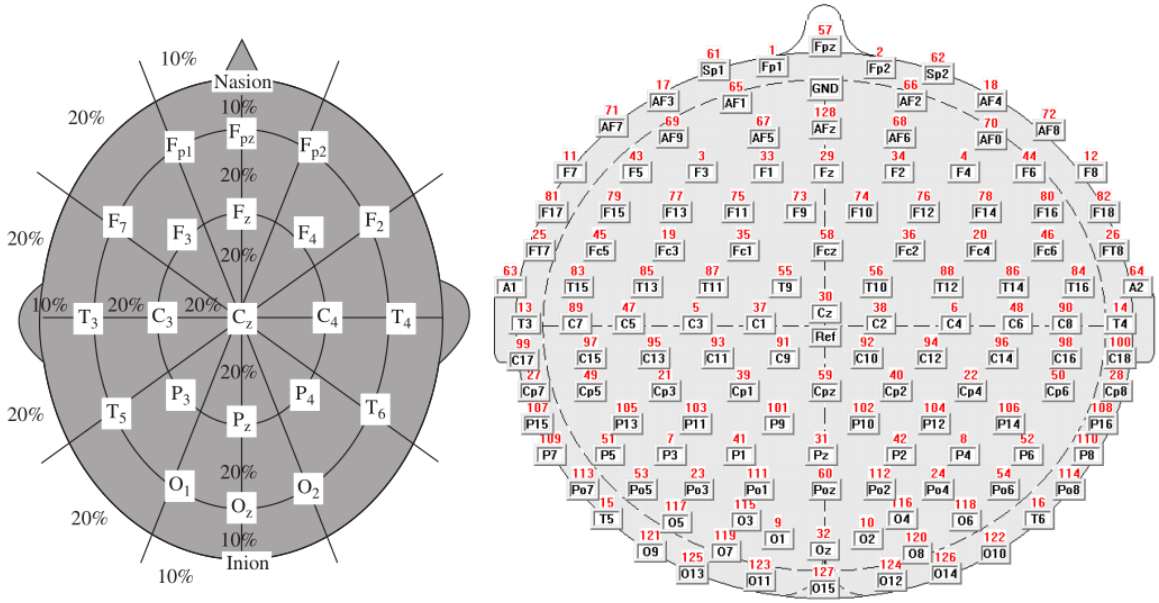

Fig. 1: Left - 10-20 standard, right - 10-20 HDEEG [6,7]

2.1.1.2 HDEEG 10-20

High-density EEG (HDEEG) is a type of scalp EEG, which uses from 64-256 monitoring electrodes (channels) to record electrical brain signals. It provides much better spatial sampling frequency (based on the number of channels used), which has been shown is crucial when estimating the source of epilepsy. The HDEEG used in this work was of upscaled 10-20 montage, as can be seen on the right side of Fig. 1. The upscaling works as follows: additional electrodes are added to the montage by their insertion equidistantly between the two original 21-channeled 10-20 montages and naming them accordingly – for example, name of a new electrode which is inserted between Cz and C3 electrodes, will be C1[6,8].

2.1.2 Invasive EEG

Invasive EEG, also known as an iEEG, is a type of EEG, where recording electrodes are in direct contact with the brain tissue. Because of the risks connected with the electrode implantation, iEEG is usually recorded only in epileptic patients, who are about to undergo a resective surgery when non-invasive localization methods are deemed as non - sufficient.

Thanks to the direct contact with the neural tissue, the invasive EEG provides a much better signal-to-noise ratio than scalp EEG. Another advantage is that the signal is much less polluted by EMG signals (*Electromyographic signals).*

2.1.2.1 ECoG

ECoG (*Electrocorticography)* is an invasive EEG procedure, where the monitoring electrodes are placed directly on the surface of the brain. The electrodes are usually arranged into a rectangular grid array or a strip. Craniotomy (removal of the part of the skull) is needed to place the electrode arrays, so this method is usually used during resective surgeries as a method of real-time resection inspection.

2.1.2.2 SEEG

SEEG (*Stereo-electroencephalography*) is a method of implanting depth electrodes deep into the brain tissue. SEEG does not give a general overview of the situation in the brain as a scalp EEG does, it provides very localized information on the implanted area of the brain as it can only derive signal in very close proximity to the electrode (distance in the order of millimeters). The placement of the depth electrodes is chosen based on the preceding scalp EEG analysis and physiological and anatomical aspects of the brain [9].

2.2 Notable EEG waveforms for epilepsy

2.2.1 IED

IEDs (also called "Spikes") are EEG markers which are traditionally used for epilepsy diagnosis [10] and for determining the scale and area of the brain region to be removed during the resective surgery if the epileptogenic zone is of focal nature. As their name suggests, IEDs occur in time intervals between seizures (hence *Interictal*). Because of their abundance, relative ease of detection and long history of being connected to epilepsy, there exists a large number of algorithms that are able to estimate the epileptogenic region of the brain or at least provide quantitative and qualitative characteristics of IEDs in some particular patient to clinical neurologist [11].

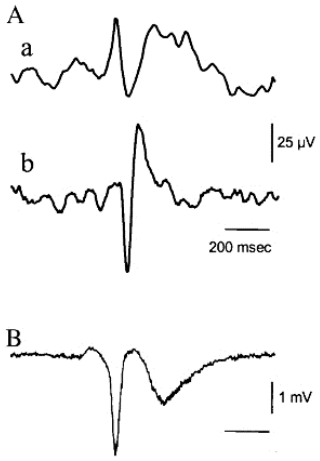

Fig. 2: Examples of Interictal Epileptic Discharges (IEDs) in time domain[10]

From the signal processing point of view, IEDs are most prominent in the frequency band of 10 – 60 Hz and generally have a duration approximately between 20 – 70 ms [12].

2.2.2 HFO

HFOs are EEG events that can be recorded outside of the classical Berger frequency band (0.5 – 30/40 Hz). The first interictal HFO events in frequency band between 80 – 500 Hz were recorded using depth microelectrodes (electrodes, which can target very small populations of neurons, diameter ~40 μm) [13],and a few years later, HFOs up to 500 Hz were recorded for the first time even through the means of macroelectrodes (surface area of ~1 mm^2) . Because of the drastic difference in the size of the HFO generating populations of neurons, it is still unclear, if HFOs recorded with micro- and macroelectrodes represent the very same phenomenon.

2.2.2.1 HFO definitions

At the time of writing of this theses, there isn't a unified definition of how an HFO should look like or what are its exact properties. But in the last few years, it seems that the general consensus regarding the HFO definition converged to the following:

HFO is a sinusoid-like signal with at least four consecutive oscillations that clearly stand out from the signal background. Then, depending on the frequency of the oscillation, an HFO is either called a *Ripple* or a *Fast ripple* [14,15].

1. Ripples (80 – 250 Hz)
2. Fast ripples (250 – 500 Hz)

Even though in most contemporary articles one can find the above-mentioned definition, every study needs to be assessed individually because of the possible differences in definition of the phenomenon and because of the possibility of actually describing different phenomena (as was said earlier, it is still not clear if HFOs recorded by various types of electrodes represent the same generation mechanism).

2.2.2.2 HFO and epilepsy

Not every EEG HFO event taking place in a frequency band between 80 – 500 Hz should be considered pathologic. There is evidence, that HFOs generally can exist outside of the epileptic network and it even seems, that in some regions of the brain (occipital region) the HFO activity should be considered normal. The physiological ripples should also show slightly different morphological characteristics – namely that physiological HFOs ought to be longer, higher in amplitude and lower in frequency, with the duration parameter being the most distinguishing feature of all listed [16].

The fact that some HFOs appear to be of physiological origin implies, that delineating regions of the brain with the highest HFO band activity as epileptic is not an optimal approach to identifying epileptic areas.

HFO on a channel can occur on a mostly flat background or emerge superimposed on an oscillatory background activity. According to [17], only resections of brain regions associated with HFO activity occurring on a channel's flat background are correlated with good surgical outcomes. Examples of presumed physiological and pathological HFOs can be seen in Fig. 3.

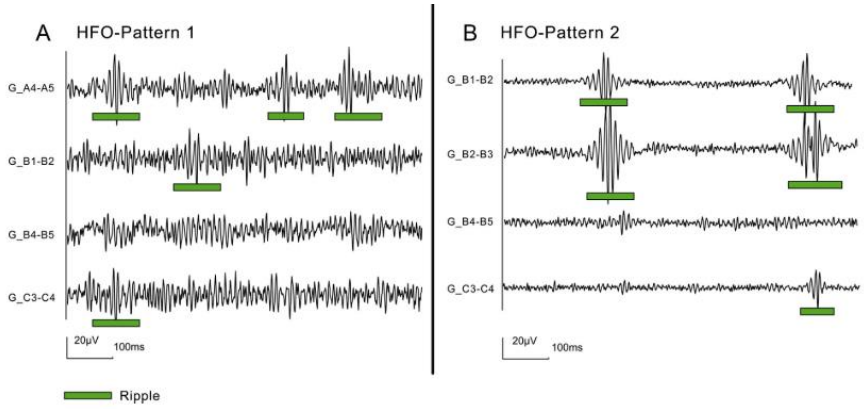

Fig. 3: A - Suspected physiological HFOs, B - suspected pathological HFOs [17]

2.2.2.3 HFO in intracranial EEG

Intracranial EEG is the best way to record artifact-free HFOs with good SNR. As the HFO oriented research progressed, researchers succeeded to record HFOs using larger and larger electrodes (from experimental microwire electrodes with diameters ~40 µm to ECoG electrodes with a surface of 7 mm). It is still not proven that HFOs gathered by various-sized electrodes represent the same process, but it is proven, that all of them are somehow connected to the epileptic brain tissue.

One of the biggest problems concerning recording HFOs with iEEG that one has to face, is the electrode placement and consequent HFO source estimation. Because of the small HFO generating volume it is hard to tell, whether the HFO signal received by the electrode originates from the position of the electrode placement or if it is a case of a propagated signal from the real HFO generating area [14].

The recommended sampling frequency for recording HFOs is at least triple the times of the maximum desired EEG frequency. This oversampling is based on the clinical experience, where the noise level in the higher frequencies overpowers any useful signal thanks to the noise generated by the EEG recording device amplifier [15].

2.2.2.4 HFO in scalp EEG

It has been proven, that it is possible to record HFOs using scalp EEG [18] and that the HFOs recorded originate in the neocortex. Originally, it was thought, that a large area of neocortex needs to be activated to propagate to the scalp – this hypothesis was proven to be false. Even focal events of small spatial extent on the brain surface can be detected on the scalp if the signal-to-noise ratio is large enough. The scalp patterns of HFOs in neocortex can be very focal, which means, that standard scalp EEG (10-20, 10-10) may undersample the scalp surface, as the estimated size of the HFO generators is ~1 cm^2[8]. This means that for a successful recording of HFOs from a scalp, it is imperative that some kind of HDEEG is used.

2.2.2.5 HFO detection methods

The fact that the HFO is not unambiguously defined, creates complications regarding its detection. Every detection scheme makes sense only if the target objective of its detection is defined beforehand. The most unifying characteristic across all scientific works done in the field of HFO phenomenon is that HFO is a wave belonging to the 80-500 Hz frequency band, with at least four oscillations noticeably stronger than the signal's background activity [19].

Visual detection (subjective)

Visual detection of HFOs is a very popular method among many HFO research teams. When used, usually the rules which were followed by the human reviewers and the conditions, under which they were carried out are listed before the rest of the presentation. An example of a visual detection methodology is following:

1. Reviewers assess the recordings simultaneously on two monitors – one with 80 Hz high pass filter applied and the other with 200 Hz high pass filter applied
2. Only events with at least 4 consecutive oscillations are labeled
3. An event is considered a ripple if visible only on the 80 Hz filtered signal and a fast ripple if only visible on the 200 Hz filtered signal [17]

Visual detection can be very accurate and create specific solutions for the epileptic zone, but it introduces subjectivity and reviewer error into the detection scheme.

Automatic detection

There has been an ongoing effort to create an automatic HFO detector, which would then go on to become an etalon across all studies concerning HFOs. Unfortunately, none of the detectors published to this day are sophisticated enough for this task. Most of the published detectors have high sensitivity but a quite low specificity. Their main problems lie in the following areas:

1. Lack of specificity
2. Lack of clear HFO definition [20]

2.2.2.6 Artifacts generated by filtering spikes

In addition to physiological HFOs, there is another class of high frequency events that do resemble pathological interictal HFOs. The filtering of an EEG signal with a high pass filter can create artifacts that are nearly impossible to tell apart from real HFOs. These HFO-like artifacts are a result of the filtering operation, which is in fact convolution of the filter impulse response and the EEG signal. If the EEG signal contains any sharp transients (for example IEDs or some kind of technical artifact), then its impulse nature will form output in the form of an impulse response of the filter, which closely resembles HFO.

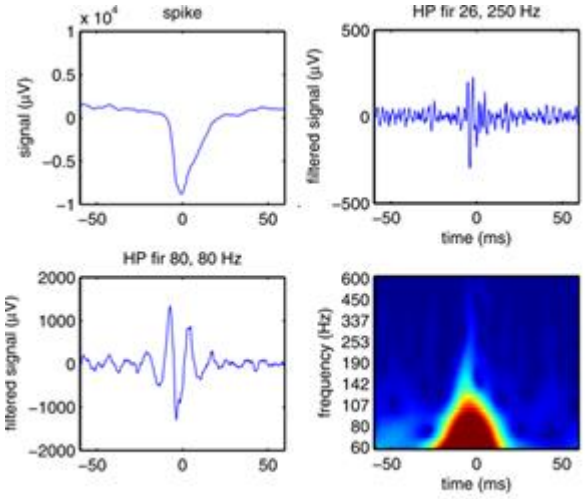

Fig. 4: Clean spike filtered by 80 and 250 Hz high pass filters, and its time-frequency analysis [21]

To combat this phenomenon, one can either check the unfiltered signal for any transients coincidental to the detected HFO, or some kind of suitable time-frequency analysis can be used. In Fig. 4, there is an example of a false HFO artifact created by high pass filtering of a transient signal. As can be seen from the figure, the time-frequency analysis shows, that this event is a case of falsely detected HFO, as only spike can be seen in the spectrogram [21].

2.2.3 Temporal relationship between HFOs and IEDs

Oscillations of higher frequencies (30 – 100Hz) occur often before IEDs in the intracranial recording of some epileptic patients. Although not a very sensitive EEG signature, it is strongly associated with electrodes in the SOZ, where the proportion of HFO active channels was higher than anywhere else [22,23].

It has been shown, that spikes which co-occur with HFO ripples in surface EEG are of shorter duration, higher amplitude and have steeper slopes. It also seems, that most of the ripples onset before the spike does and only rarely last longer than the co-occurring spike. The temporal relation between HFOs and spikes is not tightly locked, meaning, that the ripples evened out when the HFO events were averaged in time domain [24].

2.3 FCD

2.3.1 Type definition

FCD diagnosis covers a large range of possible brain malformations. As per the latest classification scheme provided by ILAE (International League Against Epilepsy), the FCD diagnosis can be divided into three following classes:

1. FCD Type I – isolated lesion with dyslamination of the neocortex
2. FCD Type II – isolated lesion with cortical dyslamination and malformed neurons/balloon cells
3. FCD Type III – focal malformation in combination with either hippocampal sclerosis or epilepsy-associated tumors [25]

2.3.2 FCD and HFOs

Generally, in all FCD patients (no matter the diagnosis type I/II/III), it seems to hold up, that the Seizure Onset Zone (SOZ) is more HFO-active then the non-SOZ areas. As the FCD type II patients show more severe malformation of brain tissue than the FCD type II patients, it has also been proved, that the HFO rates are higher in FCD type II patients when compared to FCD I (there is not enough data to at the present time to assess the relationship to FCD III patients).

The comparison of rates between FCDI/FCD II patients based on whether they are located inside or outside the SOZ can be seen in Table 1. This table has been created based upon data recorded with intracranial electrodes.

HFO rates [HFO/min]	FCD I	FCD II
SOZ channels	31.1 ± 3.6	46.5 ± 2.3
Non-SOZ channels	16.7 ± 1.5	28.7 ± 1.4

Table 1: HFO rates in FCD patients [26]

3 Methods and data

3.1 Available datasets

The EEG data used in this work are gathered in FN Motol as a part of complex examination preceding resective surgery. The EEG signals are usually recorded during the night so that the signal is mostly clear from physiological artifacts (e.g. eyeball movement, etc.). Every method and hypothesis was always developed and tried for the first time on a pilot patient P143. The patient P143 is remarkable because of the presence of very strong HFOs preceding some of the spikes. These strong HFOs can be seen very clearly with a naked eye (see Fig. 5) without the use of any filter, so there is no question of them being only filtering artifacts.

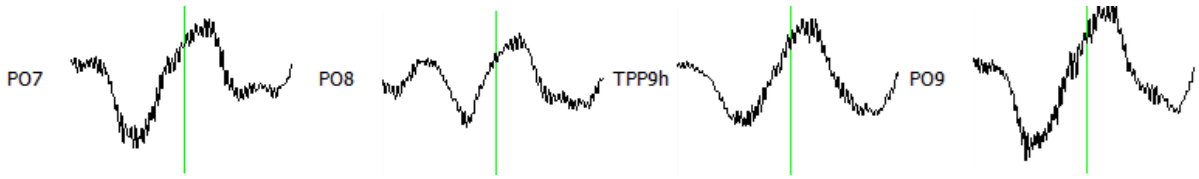

Fig. 5: Example of strong HFO+IED complex which occurs in the parietal brain region

There are two types of datasets that are analyzed in the following work. The first type of EEG data and the main target of this work are the fs = 2048Hz HDEEG data, on which general assessment of HFOs and the temporal relation of HFOs to IEDs is carried out.

The second type of EEG data is a combination of iEEG and scalp EEG recorded at the same time. The purpose of this data is to assess the temporal relationship between HFOs discovered in the iEEG and the HFOs discovered in the scalp EEG. At the time of making this work, only one dataset of this type was available – the pilot patient P143. The set up during the recording is as follows: the patient was implanted with standard SEEG with 119 channels. The suspected epileptic area was in the parietal region, so two pairs of scalp electrodes were attached to the parietal area on right and left side of the skull. Pairs of electrodes on each side of the skull were used so that they can be made into a bipolar montage, which yields one channel for left parietal side and one channel for right parietal side of the skull.

3.1.1 HDEEG

#	Patient code	Recording length [h]	Sampling frequency[Hz]	Number of channels	Diagnosis
1	P84	~9	2048	130	FCD 1
2	P125	~9	2048	130	No FCD
3	P131	~9	2048	68	N/A
4	P133	~10.5	2048	130	N/A
5	P137	~9	2048	130	N/A
6	P140	~9.75	2048	130	N/A
7	P141	~11	2048	130	N/A
8	P143	~8.5	2048	130	FCD 1
9	P152	~8.25	2048	130	N/A
10	P154	~4.5	2048	130	N/A
11	P163	~10	2048	130	N/A
12	P164	~3.25	2048	68	No FCD
13	P171	~9	2048	130	N/A
14	P174	~8	2048	130	N/A
15	P175	~9	2048	130	N/A
16	P176	~10	2048	130	N/A
17	P177	~8	2048	130	N/A
18	P178	~9.5	2048	130	N/A
19	P179	~8	2048	130	N/A
20	P183	~8.5	2048	130	N/A
21	P184	~10.5	2048	130	FCD 2
22	P186	~7	2048	130	N/A
23	P192	~9.5	2048	256	FCD 2
24	P194	~8	2048	130	N/A
25	P195	~8	2048	130	N/A

Table 2: HDEEG scalp dataset

3.1.2 iEEG + scalp electrodes

Patient code	Recording length	Sampling frequency	Number of channels
P143	~6	2048	119 (iEEG) + 4 (scalp)

Table 3: Combination iEEG + scalp electrodes dataset

3.2 Patient assessment process

The process of creating an averaged HFO event for one patient is depicted in Fig. 6. First of all, the EEG recording is visually analyzed in Alenka software, where by amplifying various frequency bands, the most prominent HFO channel (carry channel, "CC") and the HFO band is determined. The EEG recording is then run through the spike detector whose output (IED markers) are subsequently clustered (output of this sequence can be seen in Fig. 9). An aggregation of the clusterer's output is needed as every clustered event contains a spike marker for every channel. This creates a jitter effect in time because the spike markers differ in time. To combat this and create one marker for every event, all the spike markers in each event are averaged (aggregation of markers).

Data segments from the raw recording are then extracted. The usual choice for segment length is 1 second (0.5 sec before and after each marker) but otherwise is completely arbitrary. If the effect of inter-channel time jitter is too large, a synchronization of the segments takes place. The following wavelet transformation creates scalograms with a 5 Hz frequency step. Based on the information contained in the averaged time-frequency event, a patient is considered either HFO-active or inactive. If labeled as HFO-active, the patient's individual event segments are run through the HFO detector, the events with HFOs are selected and an average time-frequency HFO event is made. Otherwise a simple average of time-frequency events is made.

All of the mentioned techniques and methods are described in the rest of this chapter.

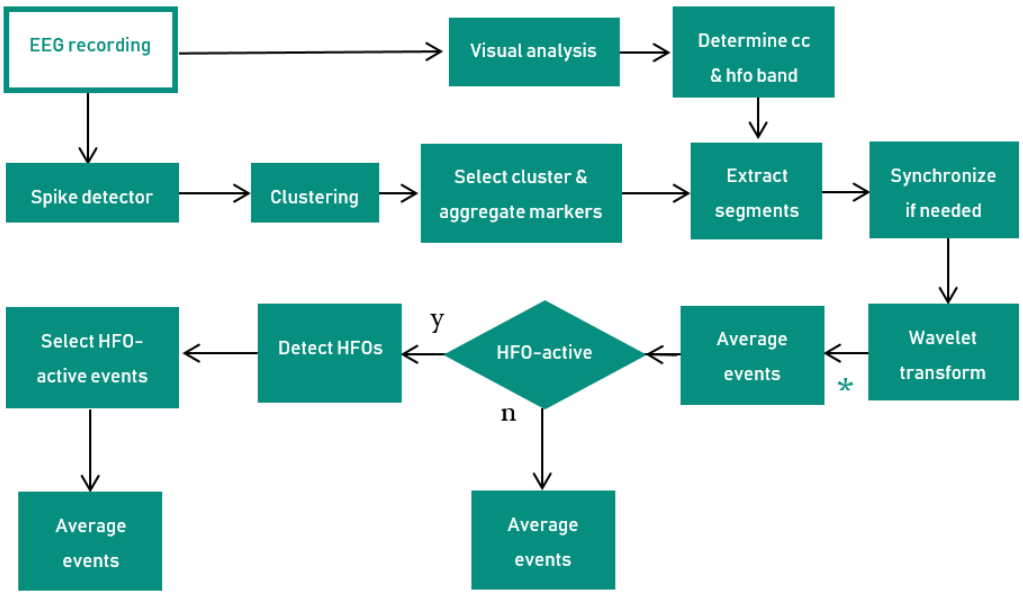

Fig. 6: Process of assessing an epileptic patient

3.3 Existing used methods and processes

3.3.1 Morlet wavelet transform

Wavelet transform similarly to Fourier transform uses a set of basis functions to expand a signal and create its projection in the frequency domain. The main difference is in the type of the used basis functions – in the wavelet transform these are not complex exponentials, but complex-valued functions called *Wavelets*.

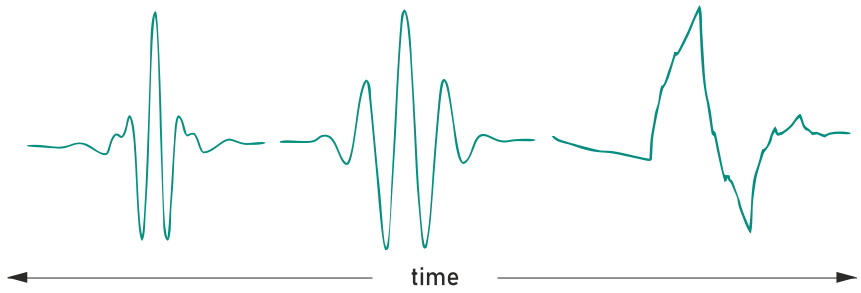

Fig. 7: Wavelet examples, left to right: Meyer, Morlet, Daubechies [27]

Wavelets come in many different types, as can be seen in Fig. 7. Each type is suitable for certain tasks and signals. For EEG signal processing, the Morlet wavelet seems to be the favorite.

The continuous wavelet transform can be defined as:

$$S(b,a) = \frac{1}{\sqrt{a}} \int_{-\infty}^{\infty} \psi' \left(\frac{t-b}{a} \right) s(t) dt$$

Continuous wavelet transform[27]

Where ψ' stands for the complex conjugated wavelet, the b parameter for the time shift of the wavelet and a parameter stands for the scale of the analyzing wavelet. The s(t) is the signal being analyzed [27].

The output of the wavelet transform creates a matrix, which is called the scalogram. Scalogram is a parallel of the spectrogram created by the STFT with one very important distinction.

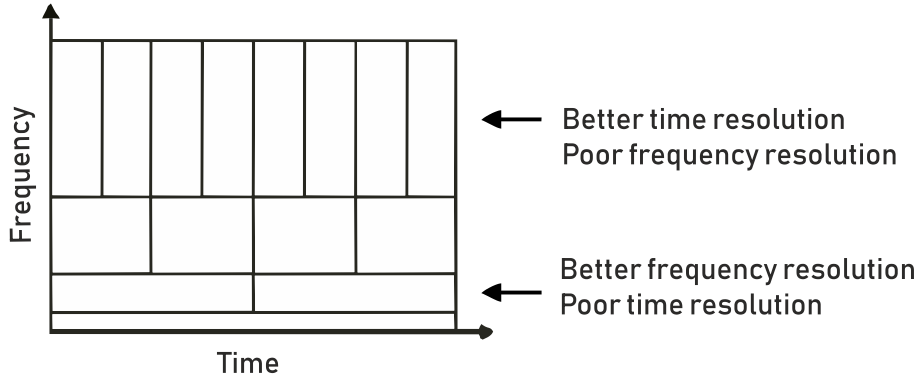

Fig. 8: Wavelet scalogram [28]

The scalogram does not have constant resolution across time and frequency as spectrogram does. As its frequency increases so does the resolution in time and as the frequency increases, the resolution in time decreases. This concept is illustrated in Fig. 8 [27,28].

3.3.2 IED detector and clustering algorithm

Since the scope of this work is restricted to researching HFOs which occur in the proximity to spikes, an extensive utilization following spike detecting and clustering algorithms took place. Both tools were always used in succession, thus spike detector's output was directly used as a spike clustering algorithm's input. The main output of these cascaded algorithms was a list of grouped population events, with every event containing spike markers for every channel. These spike-oriented methods were not developed as a part of this work, they were only used, so their description is brief in comparison to other methods down in this chapter.

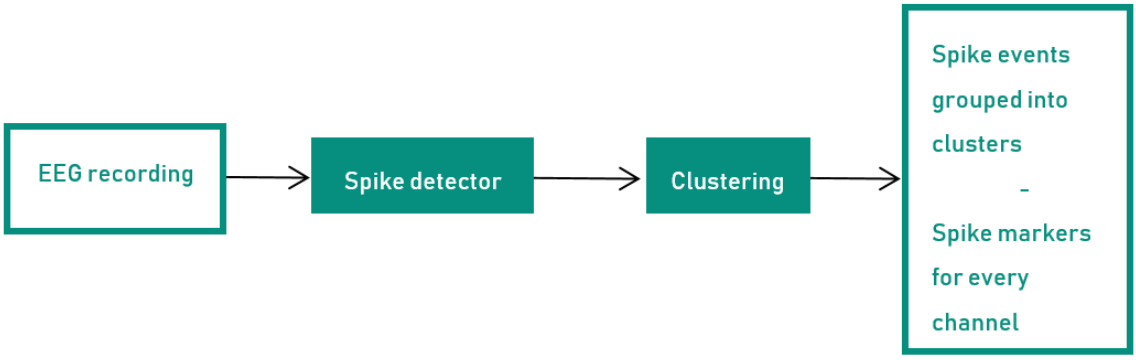

Fig. 9: Utilization of IED algorithms

3.3.2.1 Spike detector

The EEG channel in spike detector is bandpass filtered to 10-60 Hz and its envelope is computed. The signal is then segmented and for each segment, a histogram is made. Using MLE, the best fitting log-normal model is created. The presence of a spike in a signal is indicated by a positive skew of the log-normal envelope, which is caused by a larger variance in signal segment [12].

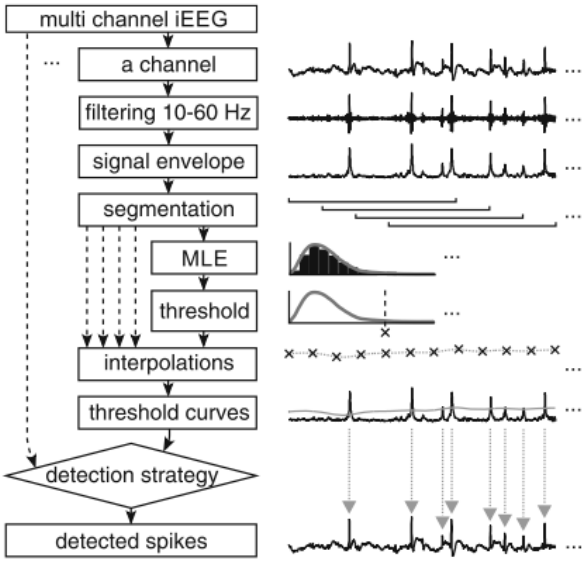

Fig. 10: Scheme of spike detector's operation [12]

3.3.2.2 Spike clustering

Because the IEDs can come in different "populations" (a certain set of channels are IED active roughly at the same time) it is possible to classify them into groups. This task is done by the spike clustering algorithm which is published here [29].

3.3.3 Alenka signal viewer

HFOs vary quite extensively among the patient cohort, so it is necessary to always perform visual analysis first to evaluate the patient's EEG record. The visual evaluation is performed with the help of the Alenka software [30]. This EEG visualization software employs many built-in functions such as pre-defined filters, which can either suppress or amplify chosen frequency band - this helps to create the desired outputs of visual analysis, which are:

1. "Are HFOs visually detectable?" → True/False
2. HFO frequency band → Frequency band in which we can expect HFOs to occur

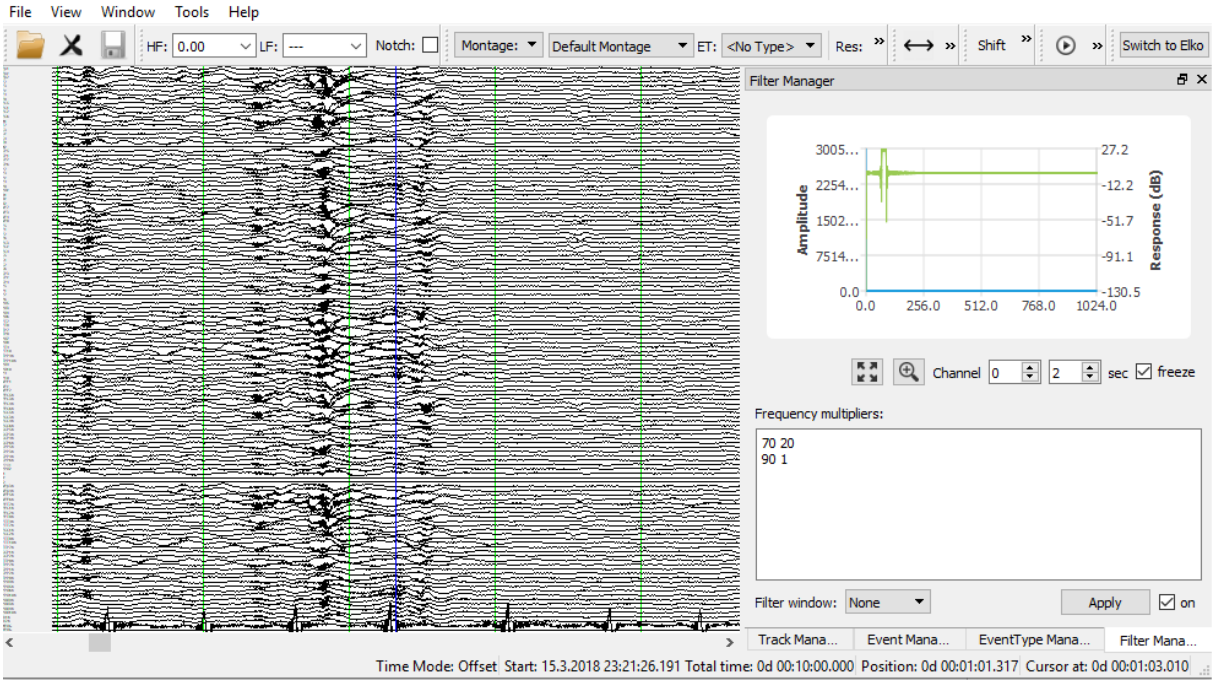

Fig. 11: Screenshot of Alenka signal viewer

3.4 Original implemented methods

3.4.1 Averaging events

To get an average HFO event that occurs in a patient, there is a need to average multiple events, where individual HFOs occur. Averaged event of any kind can provide information about the phenomenon of interest while the noise is suppressed. The averaged event can be useful among other things in two ways:

1. Averaged IED event can serve as an input into an algorithm, which tells us whether the patient has some significant HFO activity in the vicinity of an IED or not. The algorithm, that does this job with the information gathered from an averaged IED event is described in the following text.
2. It is hypothesized, that some characteristics or parameters of HFO events could help with differentiating patients with FCD diagnoses of various types. Thus an averaged HFO event for every patient is needed for further assessment and data mining.

Unfortunately, it is not possible to average HFO events in the time domain, thanks to their relative phase differences – a reference point in time to which we could lock the phase of HFOs does not exists. Averaging HFO events without phase locking them in some fashion does not yield any applicable results thanks to the destructive interference which occurs when superposing individual HFO events.

Because of the aforementioned limitation stemming from the oscillatory nature of HFOs, it is required that some kind of time-frequency decomposition is used. Wavelet transforms are much better suited for the job of EEG signal analysis, as their time resolution increases with frequency as opposed to standard STFT, where the time resolution is uniform across all frequency bins. This makes resulting scalograms much more descriptive of HFO events [31]. In this work, I have chosen the Morlet wavelet transform as Morlet wavelets are a very popular tool in EEG/MEG analysis. The process of averaging HFO events is illustrated in **Chyba! Nenalezen zdroj odkazů.**.

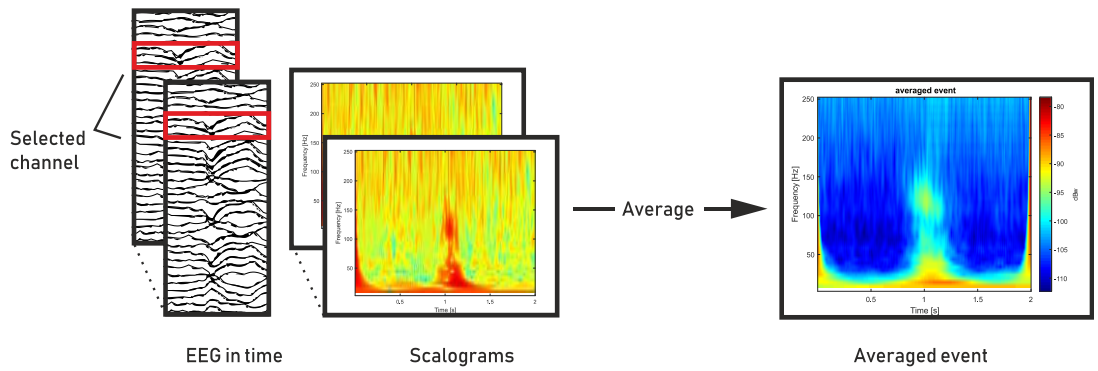

Fig. 12: Process of averaging events in time-frequency

3.4.2 Spike segments synchronization

When analyzing large sets of segments selected around the markers that are output by the spike detector, sometimes it is convenient to "synchronize" the segments in such a fashion, that the spike's extreme is positioned in the middle of the segment. This does not naturally happen because of the following reasons:

1. Every event (some unusual interesting activity across all channels e.g. a multichannel spike) output by the clustering algorithm creates multiple markers on multiple channels. These markers have some jitter to them – this means that to create one marker which would act as a center point, some kind of aggregation is needed to create one marker. We'll take the mean aggregation method as an example.
2. When we take two independent events, they have different jitter values on their respective channels. When we aggregate both mentioned independent events both resultant markers will be offset – this creates the time offset between two events and the need for some synchronization tool

For this synchronization method to work, first, a reference channel must be selected. The reference channel should be preferably the one with the highest spike and HFO rates. We select an event on this channel (1-D signal, time series) and run it through a zero-phase bandpass filter 15-35 Hz (the frequency band, where IEDs should be most prominent). The signal envelope using Hilbert's transform is then computed for the filtered signal. The envelope is then thresholded by some high quantile (e.g. 0.95).

A centroid is calculated from the parts of the envelope that made it over the threshold. The centroid acts as a first estimate of the spike location and as a kind of equilibrium point. Envelope parts over the threshold on every side of the centroid are weighted by their distance to the centroid (weighing is inverse to distance to centroid – smaller the distance to the centroid, greater the weight) and summed. The side with the bigger sum will shift the estimated IED position based on the ratio of the sums on both sides inside the interval where the occurrence of an IED is anticipated.

To synchronize full event, not only one channel, it is only needed to shift all segments in the event by the same number of samples and in the same direction as in the referential channel.

3.4.3 Detection of HFOs in spike segments

The methods for detecting HFOs described in the following sections all work with signal segments of some fixed length centered around the time marker gathered from the IED clustering algorithm. For the description to be comprehensible, the explanation is restricted to one event on one channel only.

3.4.3.1 In-band power

In this method, the input time segment is first run through a bandpass filter with manually set passband (passband is set based on manual visual assessment of patient's HFOs). The filtered time segment is divided into two main areas:

1. Area, where HFO can occur (HFO area) → adjustable time interval around a spike
2. Area, where HFO shouldn't occur (nHFO area) → everywhere else, includes segments with filter transients

Next, the HFO area is subsequently divided into three subintervals, based on their location with respect to the central point of the segment – before, over, after (see Fig. 13). For every one of these segments, a score is computed and based on the subinterval with the highest score, the HFO is then assigned to one of the groups - before, over, after and if the score is lower than some threshold, to no HFO group.

The score is computed as follows:

1. Standard deviations are computed for HFO area subinterval and for nHFO area
2. Kurtosis parameters are computed for HFO area subinterval and for nHFO area
3. Score is computed: $score = \frac{std_{HFO}}{std_{nHFO}} + \frac{kurtosis_{HFO}}{kurtosis_{nHFO}}$

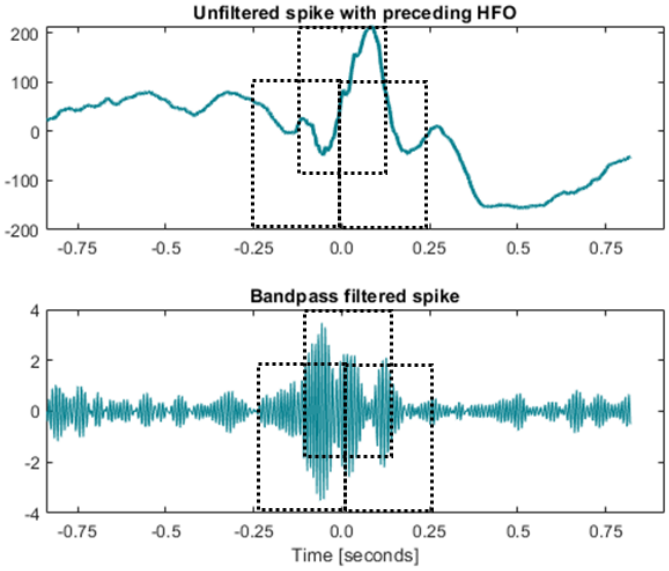

Fig. 13: Windows from which the overall HFO score is computed, in this case, the HFO is located before the spike

3.4.3.2 In-band phase

The first step of this method consists of applying Morlet wavelet transform on the signal segment. The resultant scalogram is a complex matrix that preserves the information about the signal's phase.

It seems that due to the oscillatory nature of HFOs which resembles gaussian weighted sinusoidal waveform (i.e. Morlet wavelet), the angle information obtained by the transform

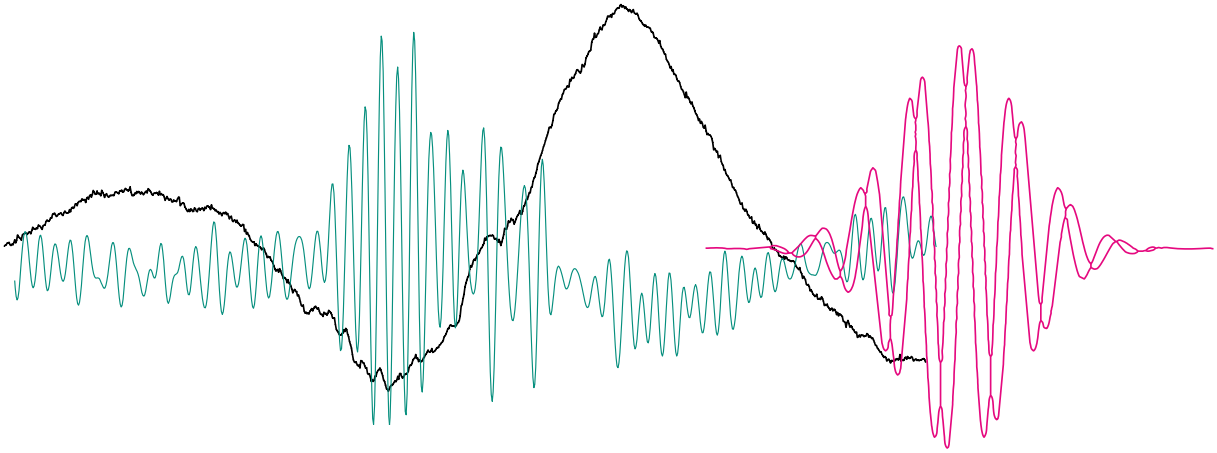

Fig. 14: Spike (black) and its superposed HFO in 100-150 Hz band (cyan), next to it is depicted the Mortlet wavelet used in wavelet transform (pink, both real and imaginary part are depicted)

should be more or less constant over the duration of the HFO event. This means that we can pinpoint all HFO-like events in the spike-containing segment by looking at the phase differences in time. So if we compute the difference of the phase for every frequency bin in the scalogram, we can then threshold the matrix with some value to create a "mask-like" binary matrix. To make thresholding easier, it is better to compute the second difference (**ΔΔθ**) as it effectively removes the DC component from the signal and thus centers the signal.

For the thresholding, to be truly fruitful, it is necessary to use various thresholds for every frequency bin there is, as the levels of noise increase approximately linearly with the frequency bins. To get around that, the threshold for every frequency bin was computed as a standard deviation of **ΔΔθ** ($\mathbf{sd}_{\Delta\Delta\theta}$) for every bin multiplied by some constant. The threshold for i-th bin is thus:

$$thr_i = k * std(\Delta\Delta\theta_i)$$

Thresholding value for i-th frequency bin in scalogram, k is an arbitrary constant

After the thresholding is complete we have a binary mask, which still has quite a lot of unwanted noise inside. To suppress it, a copy of the matrix is made, which is then shifted by a small value (e.g. 5px) in the time domain and zero padded. Following, an operation of logical AND is carried out over the original and shifted matrix – this cleans out the mask matrix so well, that we can see where the suspected HFO regions in T-F are.

The mask from the previous paragraph could be enough for masking interesting (HFO-wise) regions in the T-F space, but it is not enough to identify the position of suspected HFO in time and frequency. To estimate the position and extent of HFO in T-F space, we want to be left with a mask containing only one region. To achieve that, every bin in the cleaned-up binary scalogram mask is encoded with *Run Length Encoding* (RLE) to get every unique value and number of its repetitions (for example a sequence 11110011 will be coded as 1,0,1 (unique values) with 4,3,2 repetitions). Because we are interested only in "masked" regions we are interested only in unique values of unity and their respective repetitions. If the repetition value of a unity unique value exceeds the putative minimal duration of HFO, then the relevant sample interval in the actual bin is marked as a part of the window. When all windows for every bin are put together again to form a T-F mask, only regions with well-defined borders and next to no noise are present.

The last task is to determine, which of the regions is the one containing the HFO. We have some prior information about the HFO occurrence in time and in frequency, so we can discard regions outside the T-F region of expected occurrence. After this simple preselection, a whole range of ways of determining the HFO region opens up. One of the simplest is to just compute the power in the region and label that one as the HFO. Other approaches could make use of the shape and area of the regions.

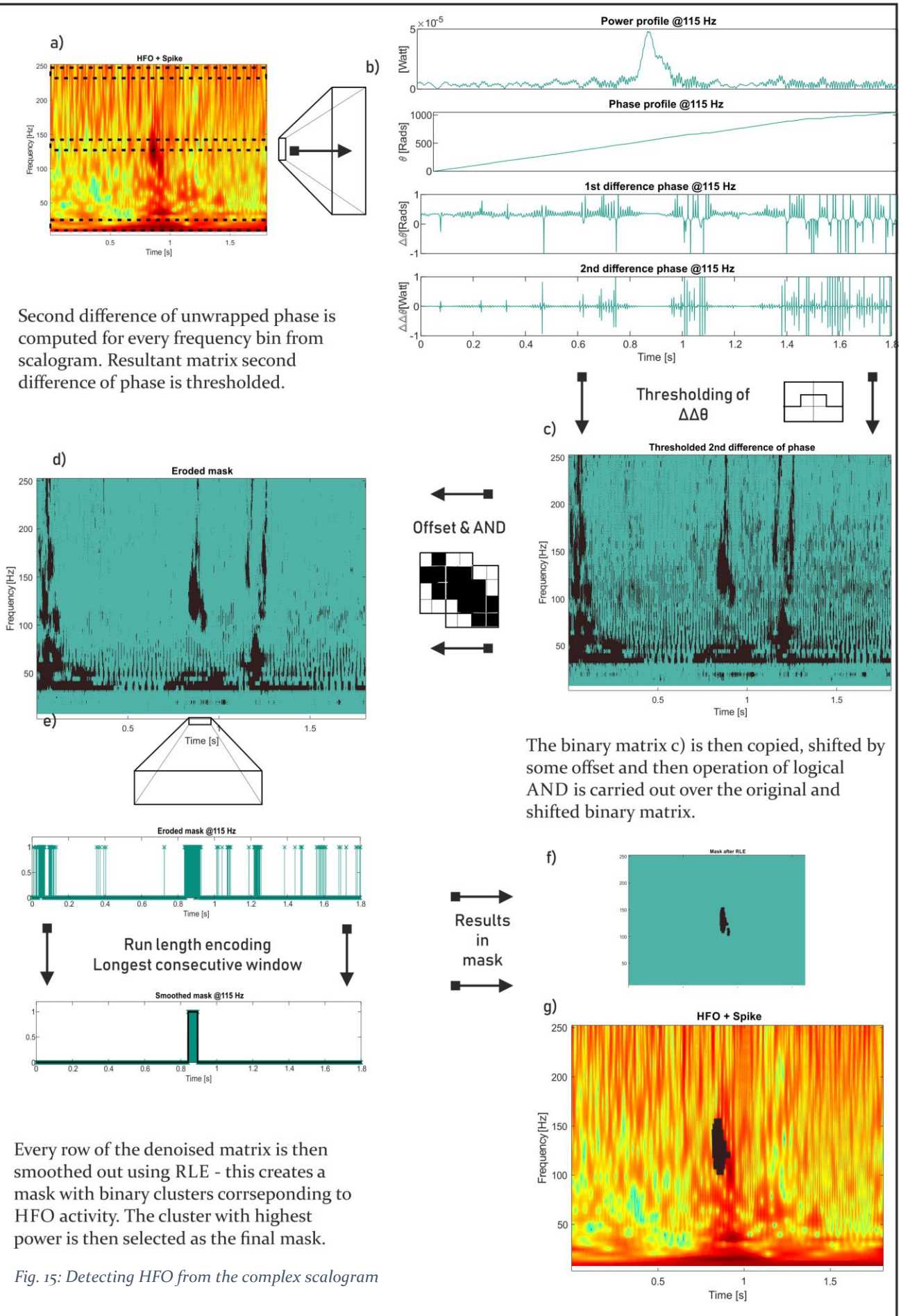

Fig. 15: Detecting HFO from the complex scalogram

3.4.4 HFO existence check

After the average HFO event is created, the first information of interest is whether the patient shows consistent HFO activity. In the ensuing text, a method is described to determine whether the patient can be labeled as “HFO active” or “HFO inactive”.

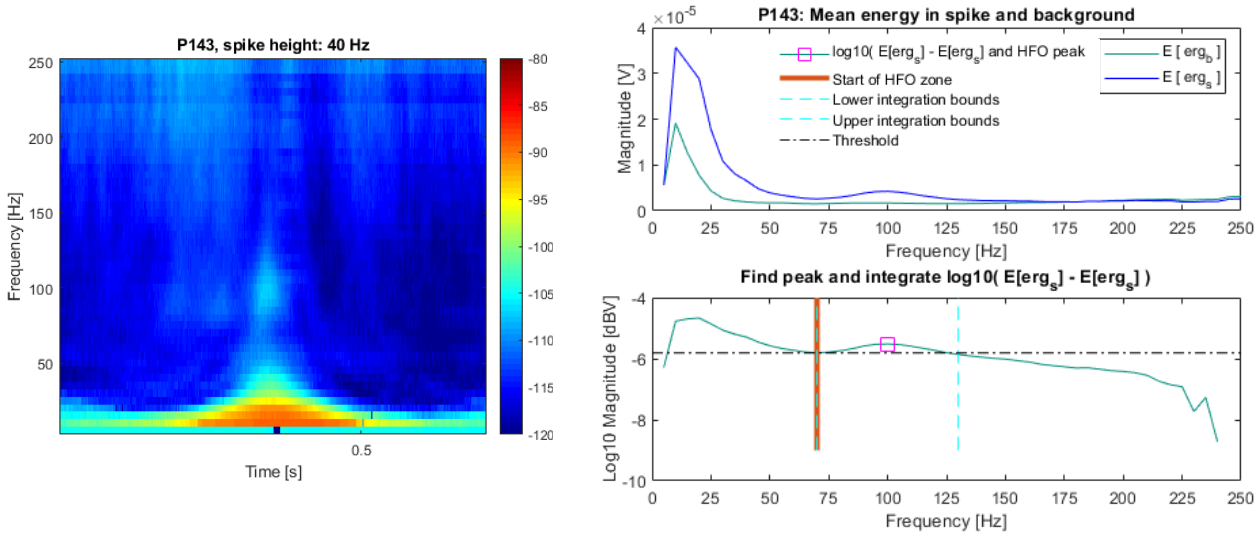

Fig. 16: Detecting HFO in averaged event

First, two energetic profiles are made, one is that of a spike and one of the signal’s background. The spike profile is made by averaging time bins in the neighborhood of the spike position and the background profile is made by averaging time bins which are not located in a spike time interval and neither in border transients created by the wavelet transform. The difference of the spike and background energy profile (hereinafter referred as to "profile"), shows the "unusualness" of the signal in the spike time interval.

Because the location of the HFO in the frequency domain is not known beforehand, we have to first determine the frequency interval in which to search. The interval for this method was defined as interval limited only from left-hand side (lower frequencies), with starting point defined as the first ensuing trough in the profile after the spike height.

To compute the spike height, the process is as follows: every frequency bin in the scalogram is centered, smoothed out by 10-tap FIR filter is thresholded by its standard deviation. The distance of the crossings of the threshold is measured in every bin to get the width of the spike and to obtain the strength of the spike in the bin, all samples over the threshold are summed and normalized. The spike profile, from which the spike height is to be inferred is then computed by weighing the distance sequence by summed samples which are over the threshold. Once the spike profile is done, the threshold used to determine the spike height is one-fifth of the maximum of the profile. The whole process is depicted in Fig. 17.

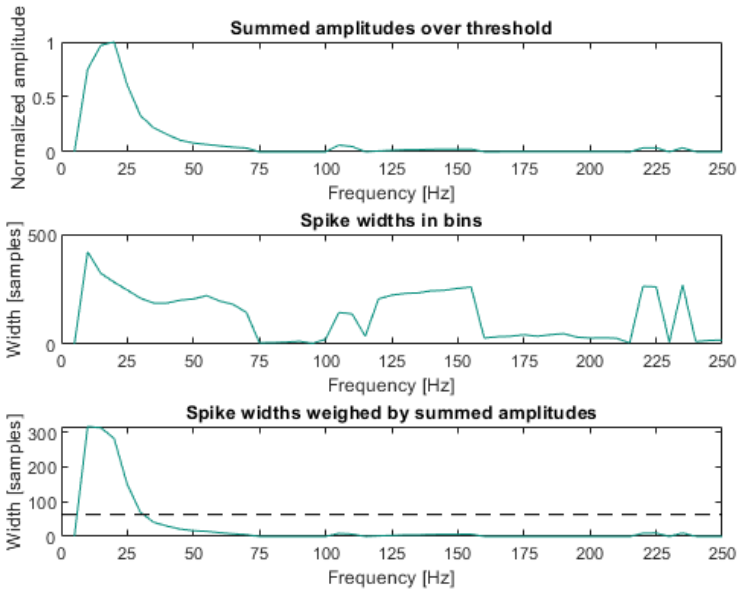

Fig. 17: Process of determining the height of the spike (P143)

The value of the profile at the start of the HFO search interval is set as a threshold value. The HFO search interval is then searched for peaks on the profile and the strongest peak is selected. If the selected peak is higher than the threshold set, it is labeled as a putative HFO of unknown prominence. The prominence is computed as an area of the peak which exceeds the threshold.

3.4.5 Assessment of temporal relation between HFOs and spikes

In this thesis, it is hypothesized, that all subjects can be split into three different groups based on their HFO-IED temporal relationship. These are:

1. Spike only – SP
2. Spikes and HFOs temporally locked - SPHL
3. Spikes and HFOs temporally not locked - SPHNL

The process of assessing if a patient shows signs of some temporal relation between the occurrence of HFO and a spike was executed as follows. First, the scalograms of EOIs (Events of Interest - segments around spikes) from the largest spike cluster are computed. Some recordings do not need any synchronization prior to scalogram computation, some do. If needed, it is imperative to synchronize the EOIs before computing scalograms as the spikes can then get spread all over the selected time interval. The scalograms are then fed to the HFO detector, which outputs the positions of HFOs in time-frequency.

To assess the temporal relation between HFO and a spike, it is essential to have the spike as centered in time as possible, so that we can use the spike as our reference point. One of the

problems that we face in this phase of the assessment task is, that the spikes are never perfectly synchronized even if the previously described synchronization algorithm is used. To assure that the spikes in our EOIs are at least somehow centered, we picked only scalograms of EOIs, whose maximum power in spike band 20-35 Hz lies on the center (±0.05 second) of the time interval. The spike band power profile was computed as a sum of the frequency bins representative of the 20-35 Hz frequency band in the respective EOI's scalogram. The reason for not picking the whole standard spike frequency band 10-50 Hz is following:

The 10-50 Hz band is all-encompassing, meaning it covers very sharp IEDs and also more "blunt", slower IEDs. The slower IEDs contain only lower frequencies and thus are not very localized especially in the scalogram, where the time resolution is worst in the lowest frequency bins. The sharp IEDs, whose frequency content can reach up to 50 Hz, are much better suited for the task of becoming a reference point. On the other hand, the energy contained in the higher frequency containers is much lower compared to the lower frequency containers. So the 20-35 Hz band can be understood as a compromise between these two mentioned restrictions.

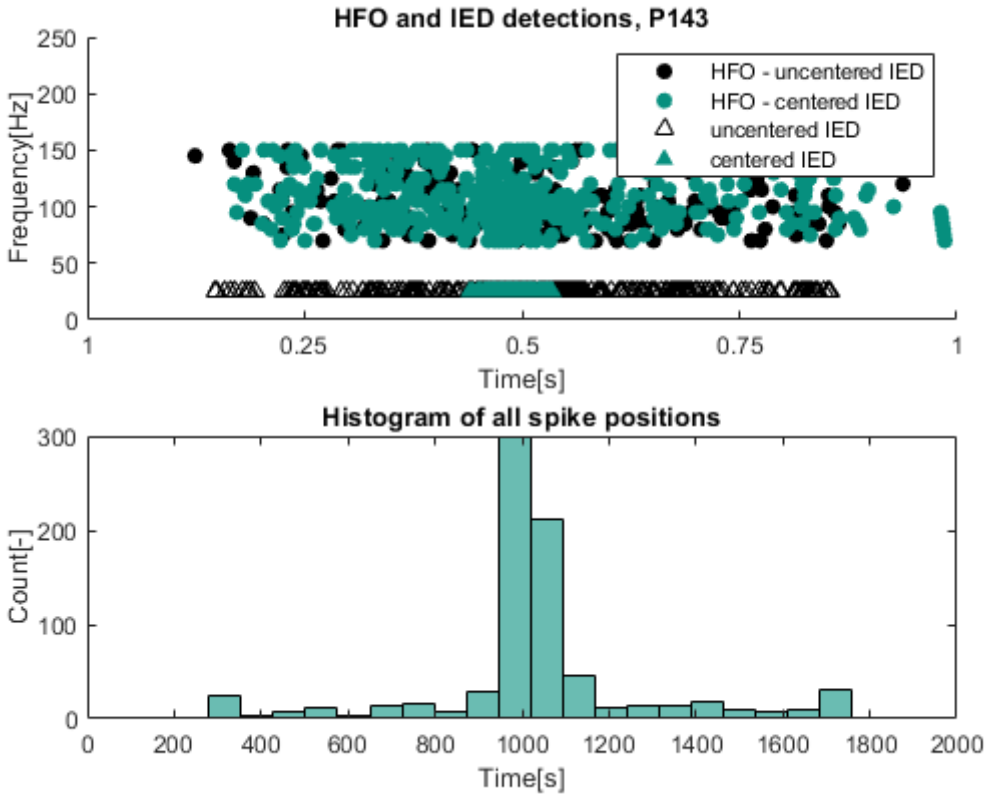

Fig. 18: Selection of HFO events corresponding to centered IEDs, top: HFO and IED positions, bottom: distribution of all IED positions

Fig. 18 depicts the situation with the majority of spikes centered their corresponding HFO positions selected (in teal). With centered EOIs and their respective HFO detections, we can do an assessment of the temporal relation of the IED and HFO phenomenon. Because we are interested in the distribution of the HFO detections in the time-frequency domain, a 2-D histogram (heat map) is created as can be seen in Fig. 19.

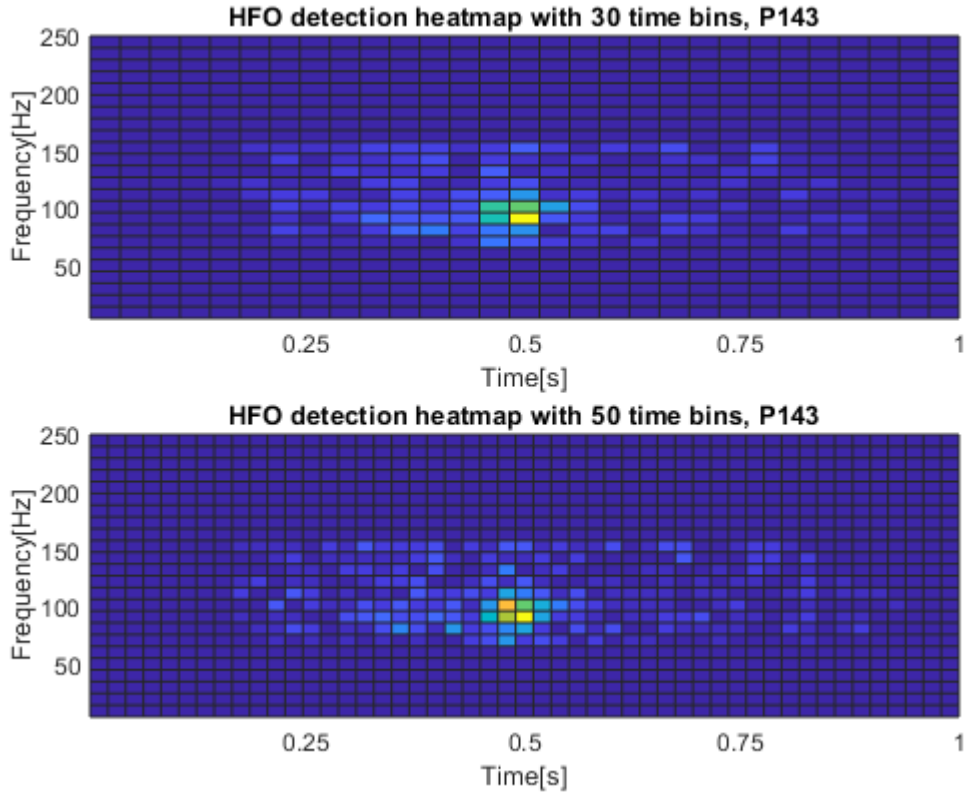

Fig. 19: Heat maps of HFO detection density, top: 30 time bins, bottom: 50 time bins

It can be seen, that the number of bins in the time dimension plays a very important role in the way, the HFO distribution in time-frequency is perceived.

To assess the relation between IEDs and HFOs in a simple and robust way and to classify HFO–active patients to group SPHL or SPHNL, an HFO "detection profile" was created for every patient by summing all frequency bins from the heat map. Basically, there are two types of profiles, which can result from summing up all frequency bins from the heat map.

1. A profile without significant maxima or peak – this profile indicates, that the HFOs and the IEDs in the particular patient do not have a significant temporal relationship (SPHNL)
2. Profile with significant maxima or peak – this profile indicates, that the HFOs and the IEDs in the particular patient could have a significant temporal relationship (SPHL)

Examples of the above-mentioned types of HFO profiles can be seen in Fig. 20. The threshold value (empirically discovered) needed to assess the type of HFO profile was computed as:

$$threshold = mean(hfo\ profile) + \frac{1}{3}(\max(hfo\ profile) - mean(hfo\ profile))$$

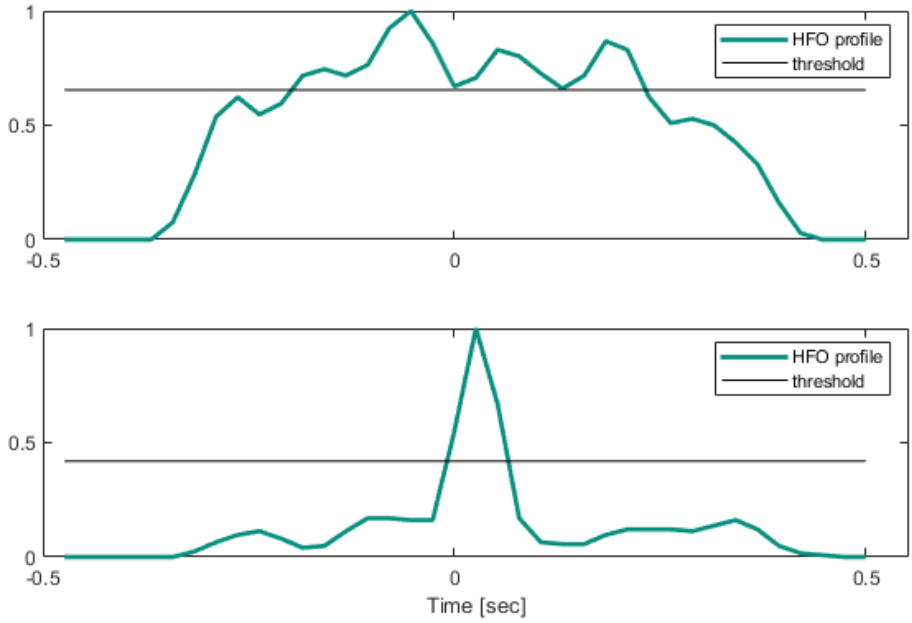

Fig. 20: HFO profiles of patients, top: SPHNL, bottom: SPHL

To separate HFO-active patients into the SPHL/SPHNL groups, the time gap between time instances, where the HFO profile exceeded the threshold value was measured.

3.5 Analysis of propagation of HFOs to the scalp

To assess the propagation of HFO events from the inside of the brain to the scalp surface, two datasets are needed – the iEEG segments containing IED + HFO and the scalp EEG segments gathered using the same timestamps as when creating the iEEG segment dataset. With these two datasets, we can observe the projection of the HFO events inside the brain to the scalp EEG.

The process of creating these two datasets is depicted in Fig. 21. First, the most HFO-active channel in the iEEG was manually found and selected and subsequently, its timestamps (acquired from the spike detector) were used to extract iEEG and scalp EEG datasets.

As the information of the occurrence of HFOs in time-frequency in pilot patient P143 is already available from the previous analysis (where in-band phase method was used), a simpler and more robust method of HFO detection inside segments was used – the in-band power method (described in 3.4.3.1). Using this in-band method, the iEEG events were split into 4 groups based on their temporal relationship between HFO and IED:

1. HFO before IED
2. HFO over IED
3. HFO after IED
4. IED without HFO

Every iEEG event's corresponding scalp EEG event was then assigned to the same group as the iEEG event. All events in all groups were then averaged in the time-frequency domain (Morlet wavelet transform). This averaging process yields the cause (inside brain) and reaction (scalp) for every group of HFOs.

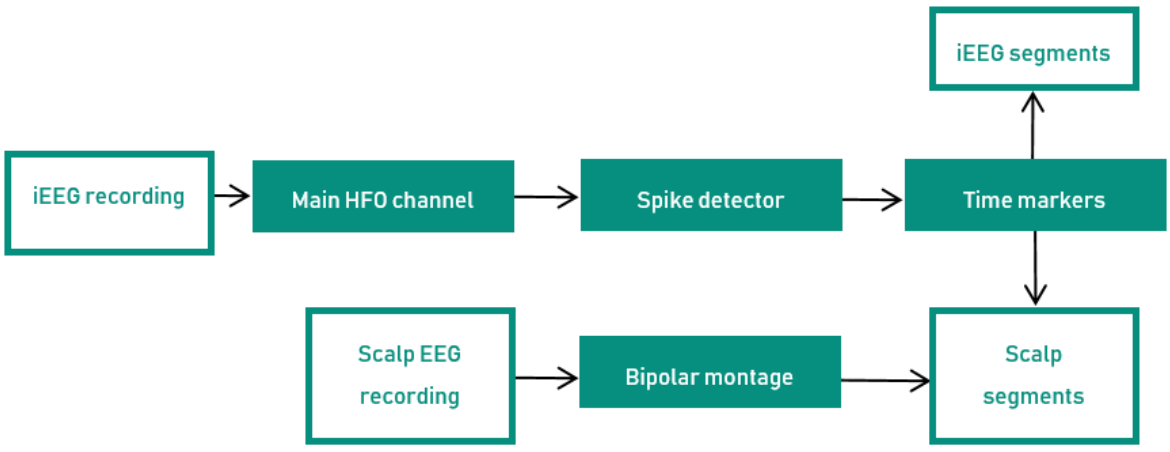

Fig. 21: Process to get corresponding iEEG and scalp EEG segments

4 Results

4.1 Patient data table

#	Patient code	HFO active		HFO profile length [temporal bins/ms]	Group	Histopathology [if available]	Epilepsy localization	
		Auto	Manual				Provided data	Author selected
1	P84	True	True	8/160	SPHNL	FCD 1	CP	CP
2	P125	True	False	10 /200	SPHNL	No FCD	CTP	CTP
3	P131	True	True	5/100	SPHL	N/A	T	T
4	P133	False	True	4/80	SP	N/A	N/A	N/A
5	P137	True	False	3/60	SPHL	N/A	N/A	N/A
6	P140	True	True	5/100	SPHL	N/A	N/A	N/A
7	P141	False	True	4/80	SP	N/A	N/A	N/A
8	P143	True	True	5/100	SPHL	FCD 1	O	PO
9	P152	True	False	5/100	SPHL	N/A	N/A	N/A
10	P154	False	False	4/80	SP	N/A	PO	CP
11	P163	True	True	4/80	SPHL	N/A	F	F
12	P164	False	True	6/120	SP	No FCD	P	P
13	P171	True	True	11/220	SPHNL	N/A	T	FT
14	P174	True	False	16/320	SPHNL	N/A	N/A	N/A
15	P175	False	False	4/80	SP	N/A	N/A	N/A
16	P176	False	True	8/160	SP	N/A	PO	FT
17	P177	False	False	5/100	SP	N/A	T	T
18	P178	True	False	10/200	SPHNL	N/A	TP	PO
19	P179	False	True	5/100	SP	N/A	TP	TP
20	P183	False	False	2/40	SP	N/A	T	P
21	P184	True	False	10/200	SPHNL	FCD 2	F	F
22	P186	False	False	4/80	SP	N/A	C	C
23	P192	False	False	11/220	SP	FCD 2	P	P
24	P194	True	False	2/40	SPHL	N/A	F	F
25	P195	False	False	4/80	SP	N/A	P	CPO

Table 4: Grouping of patients by their temporal relationship between HFO and IED. The HFO active column indicates whether the patient has been labeled as having HFOs (automatic method described in 3.4.4, manual method described in 4.2.1), the epilepsy localization data come in two versions as well – either "as provided" or the electrode which was found to be most localizing by the author was taken as referential in the "author selected" column)

4.2 Detect HFO-active patients

The average EOI scalograms obtained from the patient cohort can be separated into the following categories based on their appearance. These categories are depicted in Fig. 22 where

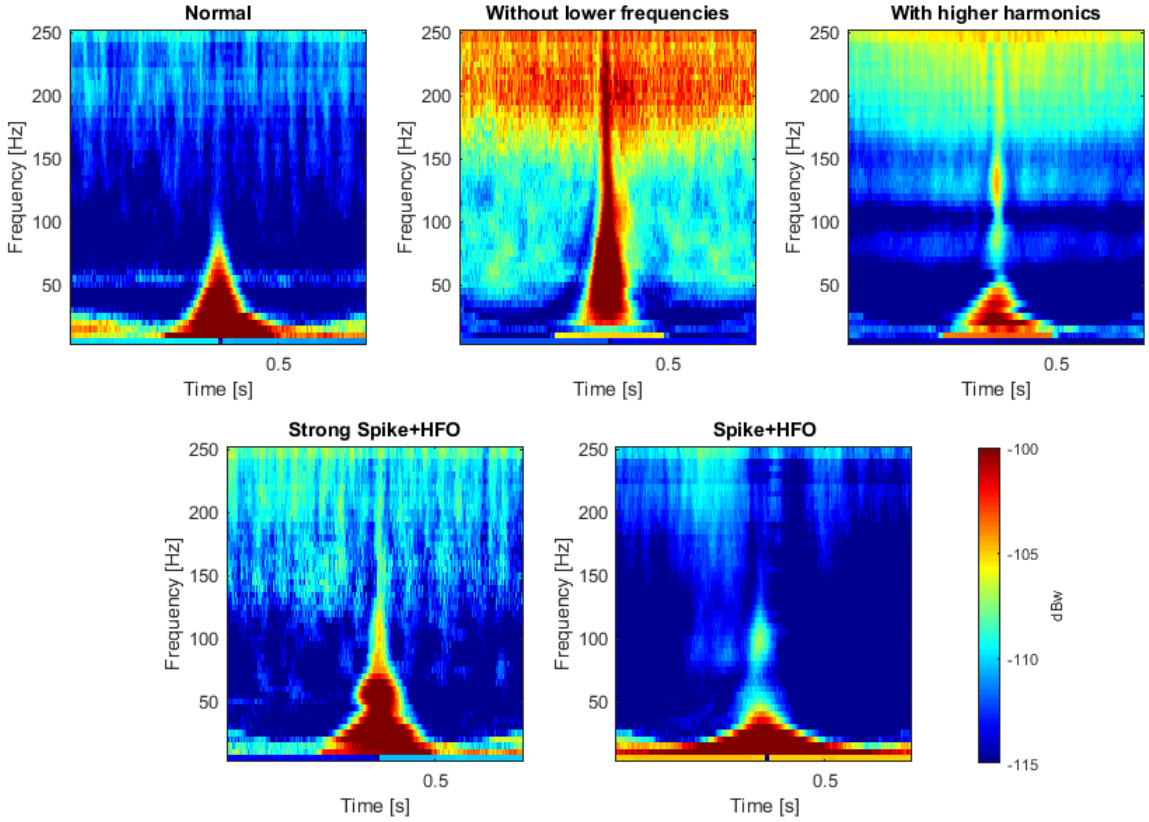

Fig. 22: Averaged EOI events separated into groups, top row: without HFO, bottom row: with HFO

the top row consists of average events that do not contain HFO activity, whereas the second row depicts average events with HFO activity.

The majority of patients who do not show HFO activity are of the *Normal* kind, that means, the spike's energy is mostly concentrated in the 0-60Hz frequency band. The spike *without lower frequencies* is a special type of averaged spike, where the energy maximum isn't in the lowest, but in higher frequencies. The last non-HFO spike version is the spike, which thanks to its temporal shape does evince higher harmonics.

The majority of patients who do show HFO activity are of the *Spike+HFO* kind, where there is a distinct trough between the spike and the HFO. Few patients evince quite strong spike activity and at the same time HFO activity which is very low in frequency (60-70Hz). This creates spikes with 'blobs' on top of them in the time-frequency.

4.2.1 Comparison to human review

To assess the performance of the detection of HFO-active patients from their average event scalogram, a comparison to the human reviewer was made. The human reviewer reference was created in the following manner: the supervisor of this thesis and author both assigned each patient's HDEEG recording into one of the following categories:

1. Clearly no HFOs
2. Perhaps no HFOs
3. Perhaps yes HFOS
4. Clearly yes HFOs

The HDEEG recordings were for the sake of the test anonymized, so neither of the reviewers knew which recording pertains to which patient. The labels from both reviewers were then aggregated to only two groups:

1. Yes HFO (mapped from clearly yes and perhaps yes)
2. No HFO (mapped from clearly no and perhaps no)

These aggregated yes/no groups were then made into a contingency table on which a Fisher's exact test was applied to find out whether the human reviewers give similar results (see Table 5). The results of the test are:

$$H = 1,\ p < 0.05$$

Supervisor\author	No	Yes
No	8	1
Yes	5	11

Table 5: Contingency table of outputs of both human reviewers, outputs are fairly consistent, but it can be seen, that supervisor shows higher sensitivity as opposed to the author

As can be seen in the preceding text, the human reviewer's outputs are fairly consistent. To create a reference to which the HFO-active patient detector will be compared, the outputs of both human reviewers were logically ANDed.

Human reference\Detector	No	Yes
No	7	7
Yes	5	6

Table 6: Contingency table of human reference vs HFO-active patient detector, it can be seen, that both methods of assessing HFOs in patient do not give the same results

The same procedure with creating a contingency table and subsequently applying Fisher's exact test was applied to evaluate the performance of the HFO detector. The Fisher's exact test did output statistically insignificant results as there is no correspondence between the human review and the detector. There may be multiple reasons for such a result, but the main suspected ones are:

1. Human reviewers consistently target different phenomenon
   As there is no clear definition at the time of writing of this thesis, it is possible, that the human reviewers and the automatic detector target different phenomenon
2. The averaging process in the averaged scalogram can suppress HFOs
   If a large number of IED events are available and at the same time, the patient's HFOs are not powerful, then the averaging process can diminish the HFO's contribution to the power scalogram and thus the patient is then falsely labeled as not HFO-active.
3. Human reviewers aren't able to recognize weak HFOs with very small amplitude
   If a large number of IED events with weak HFOs are available, the averaging process will emphasize the effect especially if the HFOs are temporally locked to the IED. This would clarify the "false positive" automatic detections.

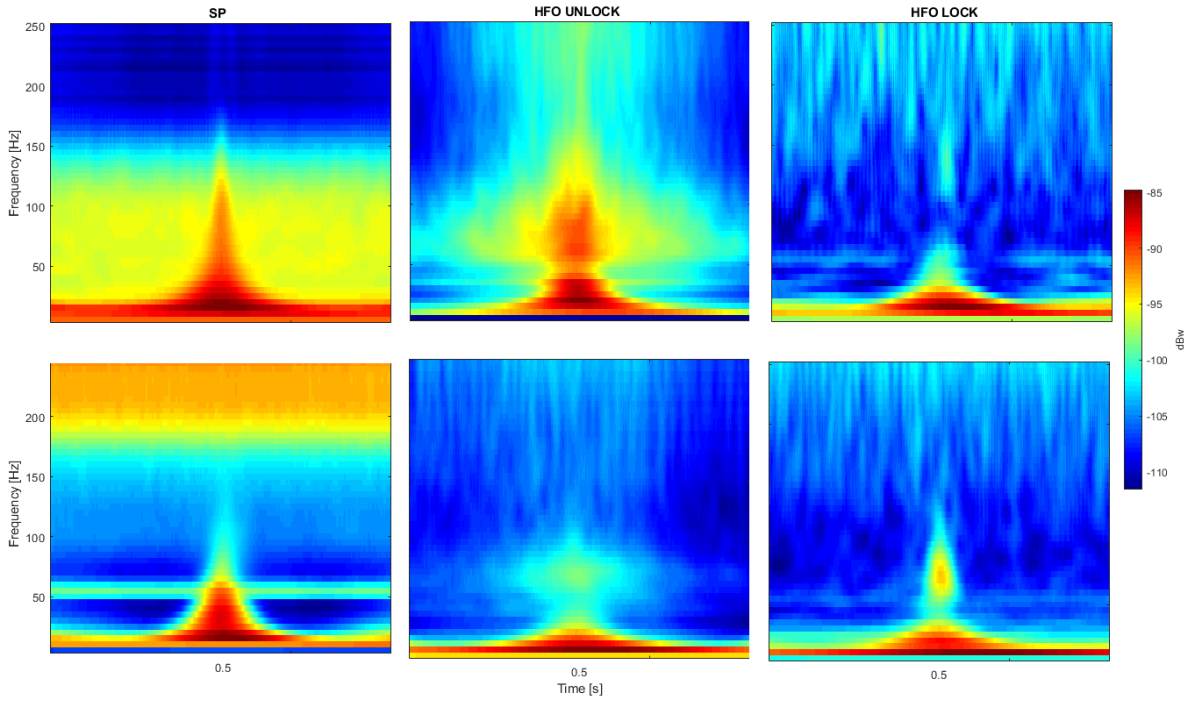

Fig. 23: Examples of classified patients, columns from left: SP, SPHNL, SPHL. The patient codes from the top left to bottom right: P154, P84, P137, P133, P171, and P163

4.3 HFOs and their temporal relation to IEDs

The stated hypothesis concerning the temporal relation of HFOs to the IEDs tells, that there should be two groups – SPHL (HFOs temporally locked) and SPHNL (HFOs temporally not locked). Because the number of HFO-active patients is quite small (13) for any meaningful statistics to be done, an empirical approach to distinguish between these two groups is needed. As mentioned in chapter 3.4.5, the number of time bins used in the heat map is a crucial parameter, which radically influences the shape of the HFO profile. For this reason, multiple heat maps with various counts of temporal bins were made for each patient. From each heat map, an HFO profile was made and the length of the HFO profile for each heat map was assessed (see the end of the chapter 3.4.5). The heat maps were created for the following temporal bin counts: 30, 40, 50, 60. The resultant histograms showing the distribution of HFO profile lengths can be seen in Fig. 24. The third configuration (number of temporal bins = 50) divides HFO-active patients the best and thus is used in dividing the patients into the SPHL/SPHNL groups.

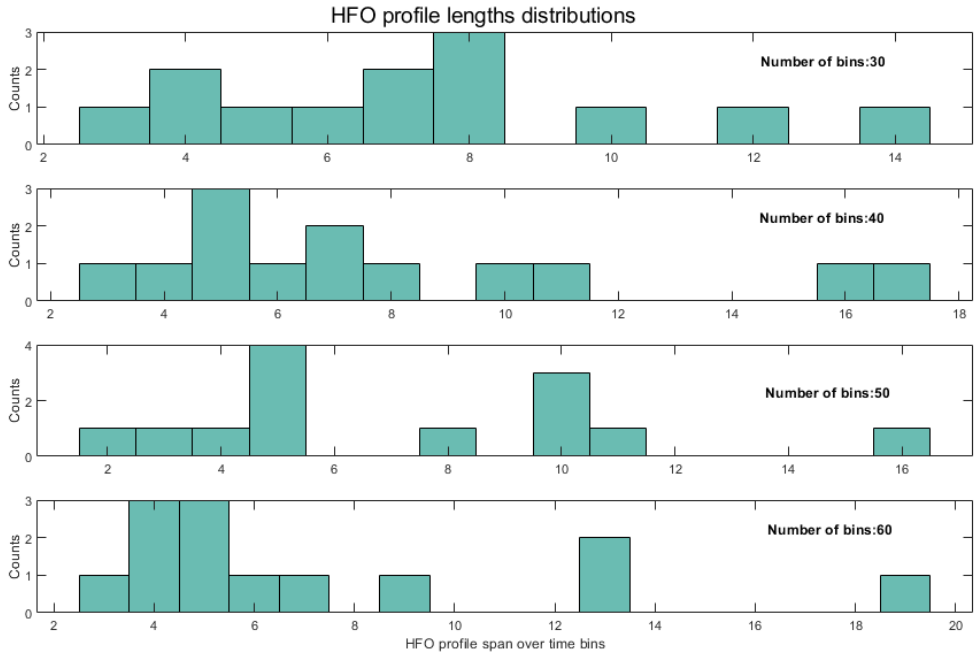

Fig. 24: Histograms of HFO profile lengths for various number of time bins in the heat map (see Fig. 19)

The boundary value used for differentiating between SPHL/SPHNL for the number of temporal bins = 50, is 6.5 (130 ms).

4.3.1 SPHL vs SPHNL

With the use of thresholding boundary value from the previous text, the 13 HFO-active patients were divided into two aforementioned groups – SPHL and SPHNL. To assess whether the division of HFO-active patients is reasonable a statistical analysis has been made.

	Mean μ [ms]	Standard deviation σ [ms]
SPHL (7 patients)	82.86	24.29
SPHNL (6 patients)	216.67	54.28

Table 7: HFO profile lengths in groups SPHL and SPHNL

For the analysis, the two sample t-test statistical test was chosen. The required sample size to combat Type II errors ($\alpha = 0.05$, power = 0.95, one-tailed test) was computed to be 2 samples for each group. With our sample sizes of 7 and 6 patients in each group, the statistical analysis should be free of Type II errors. The two sample t-test then yields the following results:

$$H = 1,\ p < 0.001$$

With this statistically highly significant result, it can be said, that there are HFO-active patients, who show the temporal relationship between some of their IEDs and HFOs recorded on their scalp.

4.4 Assess diagnosis based on HFO

To reliably determine a diagnosis of an epileptic patient, an analysis of the extracted affected brain tissue must be done. Unfortunately, thanks to the fact, that the majority of patients whose data were used in this work didn't undergo surgery yet (or even can't undergo surgery for some reason), reliable diagnoses data for the patient cohort is sparse and not sufficient to assess differences between multiple diagnoses based on the characteristics of HFOs.

The following preliminary statistics show the state of the situation when only patients for whom, diagnosis data are available at the current time (see Table 8).

	HFO profile length [temporal bins/ms]	Group	Histopathology
P84	8/160	SPHNL	FCD I
P125	10/200	SPHNL	NO FCD
P143	5/100	SPHL	FCD I
P184	10/200	SPHNL	FCD II

Table 8: HFO-active patients with available diagnostic data and their HFO profile length

The mean value of HFO profile length for FCD I is 130ms, one data point for NO FCD is 200 ms and one data point for FCD II diagnosis is 200ms. The hypothesis which would be tested

in the case all the diagnostic data would be available could be formed as follows: "HFO-active FCD I patients have a tighter temporal relationship between HFOs and IEDs".

As can be seen in Fig. 24, the boundary between temporally locked and temporally not locked HFO-active patients seems fuzzy at this time, although we can be quite sure, that there exist two populations of SPHL and SPHNL patients.

4.4.1 HFO time lock and localization

As the histopathology data aren't available yet, a substitutive clinical parameter was utilized, to ascertain, whether the classification into the SPHL and SPHNL groups gives any clinically valuable output. This alternative parameter, which is available at the moment for the majority of the patients in the cohort, is the localization of the epileptic region-to-be-resected, predicted by both neurological staff at the FN Motol hospital and by the supervisor of this thesis.

The location of interest is labeled by letters representing individual parts of the brain (F - frontal, C - central, P - parietal, O - occipital, T - temporal), or by a combination of these letters (can be seen in Table 4). As the assessment of relation between the SPHL/SPHNL groups and individual locations of interest is impossible due to the low count of data points, a simplification, where we merged all HFO-active patients whose location of interest contained parietal lobe into one group (P) and all other HFO-active patients into another (N), took place. The contingency table of this evaluation can be seen in Table 9. The number counts before the slash sign in the table cells, pertain to the provided localization data, whereas the number counts after the slash sign are a result of the analysis made by author, based upon the most localizing electrode.

[provided data/author selected]	SPHNL	SPHL
N (all non-parietal localizations)	2/2	4/3
P (all at least partly parietal localizations)	3/3	0/1

Table 9: Contingency table of HFO-IED relationship groups vs epilepsy localization groups

Application of the Fisher test on depicted contingency table does not yield statistically significant results, but the SPHL column looks very promising, when talking about the localization data provided – with larger dataset, a hypothesis could be proved, that patients who show temporal relationship between HFOs and IEDs, do not have their epileptic region localized in or on the border of parietal region. For the localization data gathered by the author, the preliminary statistic does not look very interesting, thus a much greater sample size is needed.

4.4.2 P143 – multiple temporally locked HFO populations

The pilot patient P143 shows an interesting property that has not been convincingly found in other patients from the available cohort) and that is multiple distinct HFO populations locked temporally to the spike. In patient P143, two convincingly distinct populations have been found. The two dissimilar HFO populations are different in time offset from the spike, number of events, their central frequency and in their average power. Both populations are shown in Fig. 25, where each column is an analysis of each population.

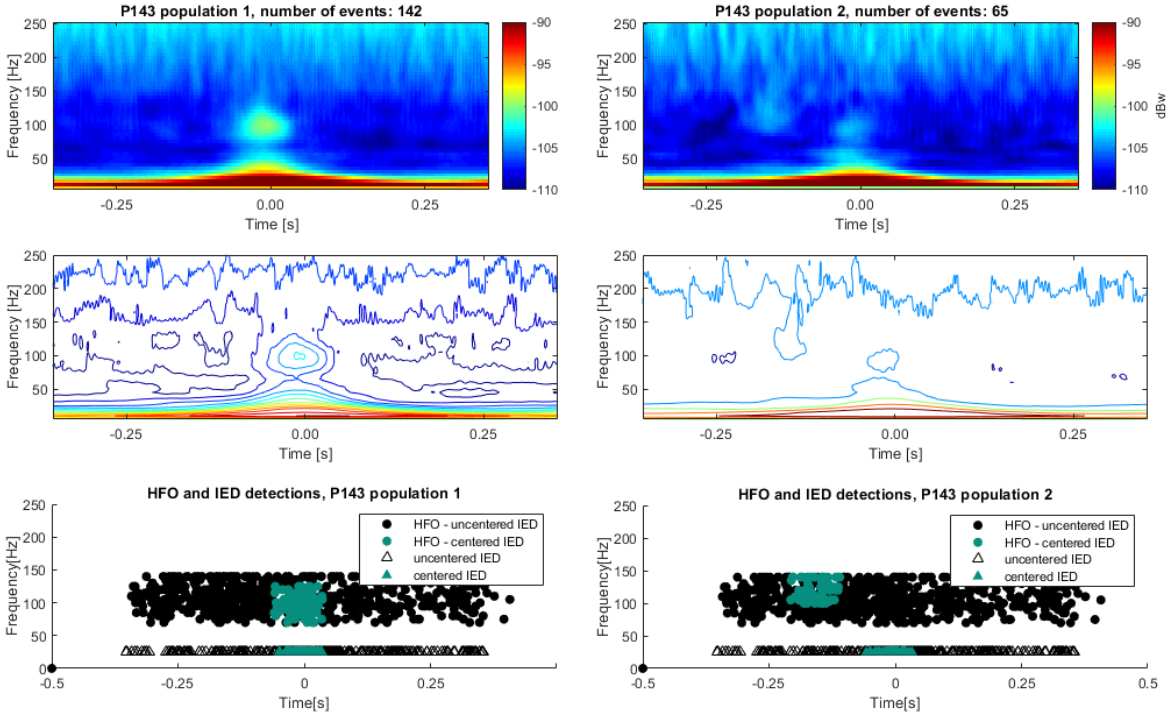

Fig. 25: Right column - HFO population occurring on top of the spike, left column - HFO population occurring before spike, top row: average scalograms of all events belonging to each of the populations, middle row: average scalograms are shown as a contour plot, bottom row: selection of only centered IED events and their appropriate HFOs forming individual HFO populations

As can be seen, the major HFO population 1 is temporally superimposed on the spike phenomenon whereas the minor HFO population 2 precedes the spike by approximately ~1/8 second, has lower amplitude, fewer events, and higher central frequency.

4.5 Relationship between intracranial and scalp HFOs – only P143

The time-frequency relationship of the HFOs recorded using iEEG and scalp EEG can be seen in Fig. 26. Every column of the graph represents one temporal relationship group where the bottom row depicts average events inside the brain (on the most HFO active electrode E9) and the top row shows the projection of the bottom row on the scalp.

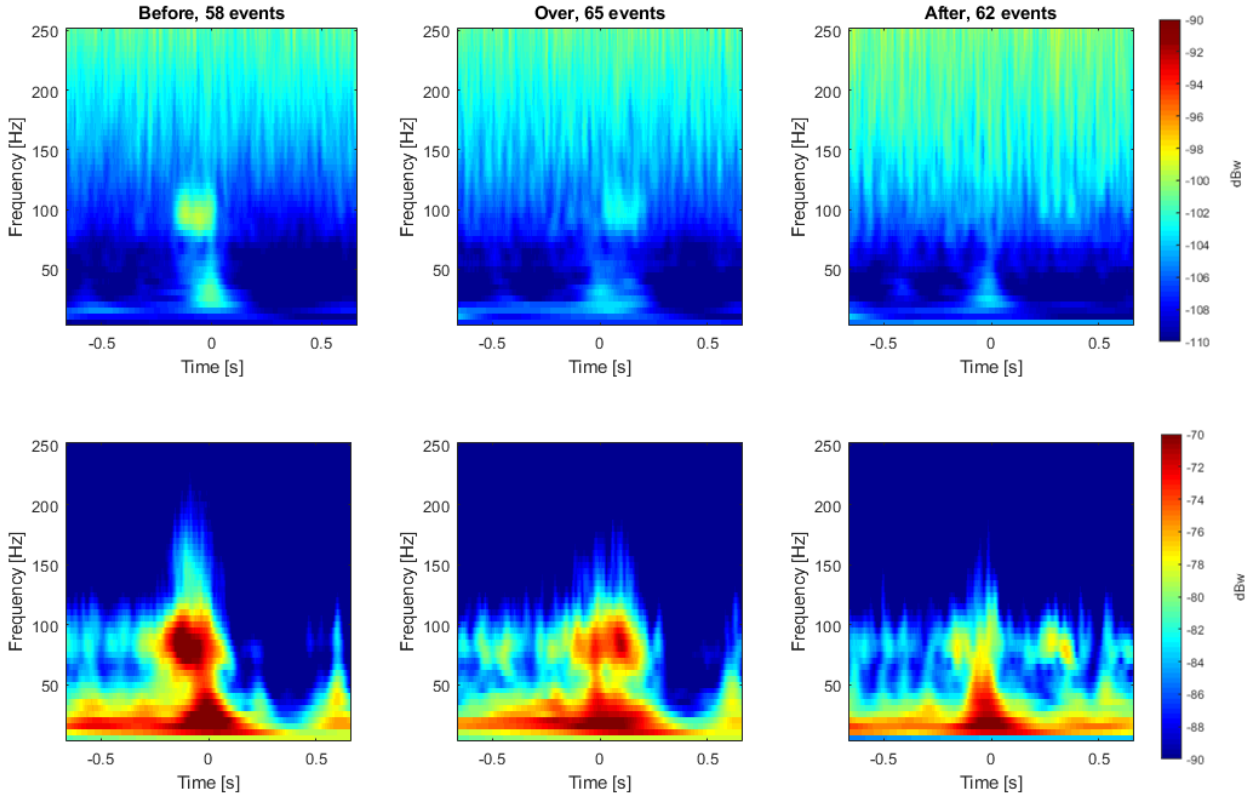

Fig. 26: Bottom - averaged grouped iEEG events, top - averaged respective scalp EEG events

No synchronization could be used in this part of the analysis, as it would damage the relationship between the inside of the brain and the scalp. The consequence is that the spikes are less well defined in the time-frequency domain as can be seen on the example of the group *Over* where the spike is evidently not as well defined as in group *Before*.

To assess the delay between the intracranial and scalp HFOs, temporal cross-sections of time-frequency scalograms were made at frequency bin corresponding to the HFO central frequency (100 Hz in the case of pilot patient P143) for every group. These normalized cross-sections are depicted in Fig. 27, where iEEG and scalp EEG power profile is represented by teal and black color respectively.

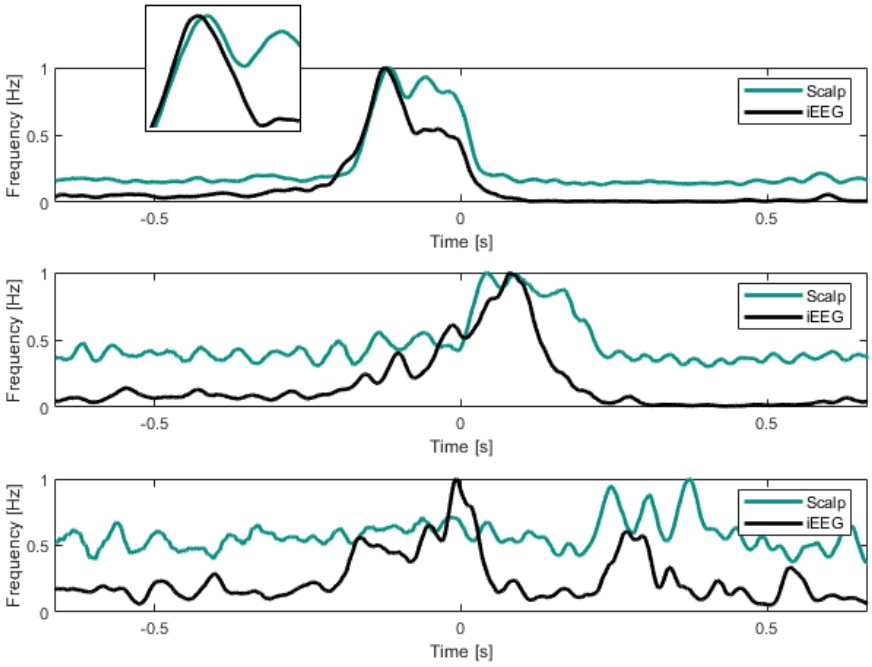

Fig. 27: Normalized power profiles @ 100 Hz (HFO central frequency), top to bottom: before, over, after

The *Before* group shows the correspondence between the inside of the brain and the scalp the best. The iEEG rising slope before the maximum peak has slight lead time to the maximum peak of scalp EEG. These correlated peaks with a slight delay between each other strongly indicate, that some HFOs which can be recorded inside the brain find a way through the skull tissue so that they can be captured by scalp EEG.

The *Over* group shows the same effect, but not in such a clean manner. The *After* group's effect of propagation to the scalp doesn't seem to be very prominent.

5 Conclusion

With the goal of meeting the thesis's assignments, new signal processing methods were devised including the IED event synchronization algorithm and two HFO detectors using different approaches. The detector of HFO activity didn't perform well at all when compared to human reviewers, but at the same time didn't act nonsensically as can be seen in Fig. 23. The in-band power HFO detection scheme allowed for a robust assessment of the relationship between HFOs recorded with intracranial electrodes and HFOs recorded with scalp electrodes. The in-band phase HFO detector allowed for a general assessment of the presence of HFOs in individual patients.

In this work, it has been shown, that events which can be labeled as HFOs (activity in frequency band 80-500 Hz with at least four oscillations over the channel's background power threshold), can be found in some epileptic patient's HDEEG scalp recording, in the vicinity of IEDs. Thirteen patients out of twenty-five datasets overall were labeled as HFO-active. The HFOs detected in HFO-active patients have shown differing characteristics like average amplitude, central frequency, and duration.

To make the assessment of the temporal relation between HFOs and IEDs as simple as possible, two groups were devised to sort the HFO-active patients into – the SPHL and SPHNL. The first group is made up of patients whose HFOs seems to be temporally locked to the IED and the second group is made up of patients whose HFOs seems to not be temporally locked to the IED. From 13 HFO-active patients, 6 was labeled as SPHNL and the remaining 7 as SPHL. The statistical analysis of the HFO profile length, on which the distinction between these two groups was made, did turn out with $p < 0.001$.

A promising preliminary statistics comparing SPHL/SPHNL groups against the localization data regarding the epileptic region-to-be-resected was carried out. The results of these statistics indicate, that patients who show signs of temporal relationship between HFOs and IEDs do not have their epileptic area located in or bordering with the parietal region. For the statistic to be more convincing, a larger sample size is needed in future.

Unfortunately, thanks to the nearly non-existent histology data for the patient cohort used, it is impossible to verify any scheme of differentiating between FCD I and FCD II based upon the HFO biomarker. This thesis can, however, help in future works with the goal of differentiating FCD types, as soon as the histology data is finally available.

Pilot patient P143 showed not negligible evidence, that it is possible for one patient to evince such HFO activity, that individual HFO events can be grouped into multiple categories based on their time-frequency properties. Particularly in P143, two populations of HFOs were

found - the major population (with roughly twice more individual HFO events), whose events occurred on frequency ~100 Hz approximately at the same moment as relevant IED, and the minor population, whose events occurred on higher frequency ~130 Hz and with a lead time of ~0.125 s before the relevant IED.

For the lack of more datasets, which combine simultaneous intracranial recording with selected scalp electrodes, only the pilot patient's (P143) dataset was evaluated. The result of this dataset's analysis was twofold. The incidental result was the confirmation of the existence of the HFOs detected in the HDEEG data of the same patient, as the same HFOs were found in the left parietal scalp electrode of the combined dataset. Subsequently, the main result was the fact, that some HFOs which are recorded by the intracranial electrodes propagate to the scalp.

6 References

1. Fisher RS, Acevedo C, Arzimanoglou A, et al. ILAE Official Report: A practical clinical definition of epilepsy. *Epilepsia*. 2014;55(4):475-482. doi:10.1111/epi.12550
2. Pang T, Atefy R, Sheen V. Malformations of Cortical Development. *Neurologist*. 2008;14(3):181-191. doi:10.1097/NRL.0b013e31816606b9
3. Oppenheim A V., Schafer RW. *DISCRETE-TIME SIGNAL PROCESSING*. Upper Saddle River, New Jersey 07458: Prentice hall; 1998.
4. Lantz G, Grave de Peralta R, Spinelli L, Seeck M, Michel C. Epileptic source localization with high density EEG: how many electrodes are needed? *Clin Neurophysiol*. 2003;114(1):63-69. doi:10.1016/S1388-2457(02)00337-1
5. Marmor O, Valsky D, Joshua M, et al. Local vs . volume conductance activity of field potentials in the human subthalamic nucleus. 2017;c:2140-2151. doi:10.1152/jn.00756.2016
6. Sanei S, Chambers JA. *EEG SIGNAL PROCESSING*. John Wiley & Sons Ltd; 2007.
7. *Comfort Testing Project Report*. USA; 2014.
8. Zelmann R, Lina JM, Schulze-Bonhage A, Gotman J, Jacobs J. Scalp EEG is not a blur: It can see high frequency oscillations although their generators are small. *Brain Topogr*. 2014;27(5):683-704. doi:10.1007/s10548-013-0321-y
9. Noachtar S, Rémi J. The role of EEG in epilepsy: A critical review. *Epilepsy Behav*. 2009;15(1):22-33. doi:10.1016/j.yebeh.2009.02.035
10. de Curtis M, Avanzini G. Interictal spikes in focal epileptogenesis. *Prog Neurobiol*. 2001;63(5):541-567. doi:10.1016/S0301-0082(00)00026-5
11. Wilke C, Drongelen W van, Kohrman M, He B. Identification of epileptogenic foci from causal analysis of ECoG interictal spike activity. *Clin Neurophysiol*. 2009;120(8):1449-1456. doi:10.1016/j.clinph.2009.04.024
12. Janca R, Jezdik P, Cmejla R, et al. Detection of Interictal Epileptiform Discharges Using Signal Envelope Distribution Modelling: Application to Epileptic and Non-Epileptic Intracranial Recordings. *Brain Topogr*. 2014;28(1):172-183. doi:10.1007/s10548-014-0379-1
13. Bragin A, Engel J, Wilson CL, Fried I, Buzsáki G. High-frequency oscillations in human brain. *Hippocampus*. 1999;9(2):137-142. doi:10.1002/(SICI)1098-1063(1999)9:2<137::AID-HIPO5>3.0.CO;2-0
14. Jacobs J, Staba R, Asano E, et al. High-frequency oscillations (HFOs) in clinical epilepsy. *Prog Neurobiol*. 2012;98(3):302-315. doi:10.1016/j.pneurobio.2012.03.001
15. Zijlmans M, Worrell GA, Dümpelmann M, et al. How to record high-frequency oscillations in epilepsy: A practical guideline. *Epilepsia*. 2017;58(8):1305-1315.

doi:10.1111/epi.13814

16. Alkawadri R, Gaspard N, Goncharova II, et al. The spatial and signal characteristics of physiologic high frequency oscillations. *Epilepsia*. 2014;55(12):1986-1995. doi:10.1111/epi.12851
17. Kerber K, Dümpelmann M, Schelter B, et al. Differentiation of specific ripple patterns helps to identify epileptogenic areas for surgical procedures. *Clin Neurophysiol*. 2014;125(7):1339-1345. doi:10.1016/j.clinph.2013.11.030
18. Kobayashi K, Watanabe Y, Inoue T, Oka M, Yoshinaga H, Ohtsuka Y. Scalp-recorded high-frequency oscillations in childhood sleep-induced electrical status epilepticus. *Epilepsia*. 2010;51(10):2190-2194. doi:10.1111/j.1528-1167.2010.02565.x
19. Frauscher B, Bartolomei F, Kobayashi K, et al. High-frequency oscillations: The state of clinical research. *Epilepsia*. 2017;58(8):1316-1329. doi:10.1111/epi.13829
20. Roehri N, Pizzo F, Bartolomei F, Wendling F, Bénar CG. What are the assets and weaknesses of HFO detectors? A benchmark framework based on realistic simulations. *PLoS One*. 2017;12(4):1-20. doi:10.1371/journal.pone.0174702
21. Bénar CG, Chauvière L, Bartolomei F, Wendling F. Pitfalls of high-pass filtering for detecting epileptic oscillations: A technical note on "false" ripples. *Clin Neurophysiol*. 2010;121(3):301-310. doi:10.1016/j.clinph.2009.10.019
22. Ren L, Kucewicz MT, Cimbalnik J, et al. Gamma oscillations precede interictal epileptiform spikes in the seizure onset zone. *Neurology*. 2015;84(6):602-608. doi:10.1212/WNL.0000000000001234
23. Andrade-Valenca LP, Dubeau F, Mari F, Zelmann R, Gotman J. Interictal scalp fast oscillations as a marker of the seizure onset zone. *Neurology*. 2011;77(6):524-531. doi:10.1212/WNL.0b013e318228bee2
24. van Klink N, Frauscher B, Zijlmans M, Gotman J. Relationships between interictal epileptic spikes and ripples in surface EEG. *Clin Neurophysiol*. 2016;127(1):143-149. doi:10.1016/j.clinph.2015.04.059
25. Blümcke I, Thom M, Aronica E, et al. The clinicopathologic spectrum of focal cortical dysplasias: A consensus classification proposed by an ad hoc Task Force of the ILAE Diagnostic Methods Commission. *Epilepsia*. 2011;52(1):158-174. doi:10.1111/j.1528-1167.2010.02777.x
26. Kerber K, Levan P, Dümpelmann M, et al. High frequency oscillations mirror disease activity in patients with focal cortical dysplasia. *Epilepsia*. 2013;54(8):1428-1436. doi:10.1111/epi.12262
27. Lee DTL, Yamamoto A. Wavelet analysis: theory and applications. *Hewlett-Packard J*.

1994;45:44-54. http://www.hpl.hp.com/hpjournal/94dec/dec94a6.pdf.

28. Tadel F, Pantazis D, Bock E, Baillet S. Brainstorm tutorials: Time-frequency. Brainstorm Tutorials. https://neuroimage.usc.edu/brainstorm/Tutorials. Published 2017. Accessed February 8, 2019.
29. Janca R. The sub-regional Functional Organization of neocortical irritative epileptic networks in Pediatric epilepsy. 2018;9(March):1-11. doi:10.3389/fneur.2018.00184
30. Bárta M. Multiplatformní zobrazovací software pro elektroencefalografii. 2018.
31. Roach BJ, Mathalon DH. Event-Related EEG Time-Frequency Analysis : An Overview of Measures and An Analysis of Early Gamma Band Phase Locking in Schizophrenia. 2008;34(5):907-926. doi:10.1093/schbul/sbn093

Appendix A DVD Content

- Funs - directory with necessary .m functions
- Demo_P143.m - demo m-file (SPHL example)
- Demo_P125.m - demo m-file (SPHNL example)

Appendix B Table of abbreviations

CC	Carry channel
ECoG	Electrocorticography
EEG	Electroencephalography
EMG	Electromyography
FCD	Focal cortical dysplasia
HDEEG	High-density EEG
HFO	High frequency oscillation
IED	Interictal epileptiform discharge
iEEG	Intracranial EEG
MCD	Malformations of cortical development
MLE	Maximum likelihood estimation
RLE	Run-length encoding
SEEG	Stereo electroencephalography
SNR	Signal to noise ratio
SOZ	Seizure onset zone
SP	Spike only group
SPHL	Spike HFO locked group
SPHNL	Spike HFO not locked group
STFT	Short-time Fourier transform
T-F	Time-frequency domain